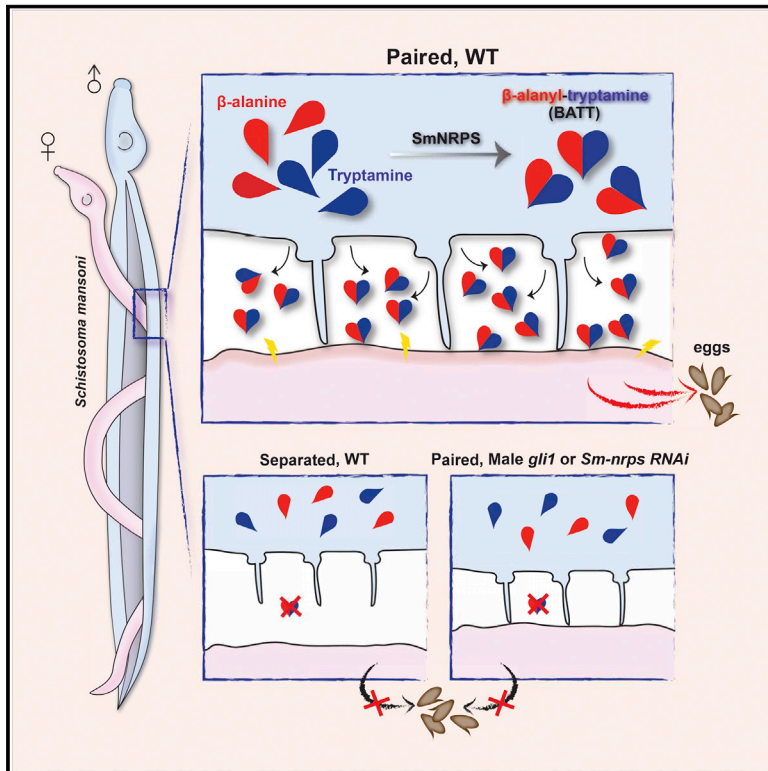


# A male-derived nonribosomal peptide pheromone controls female schistosome development

## Graphical abstract



## Authors

Rui Chen, Jipeng Wang, Irina Gradinaru, ..., Ralph J. DeBerardinis, Elliott M. Ross, James J. Collins III

## Correspondence

jamesj.collins@utsouthwestern.edu

## In brief

A nonribosomal peptide produced by male schistosomes when paired with a female is responsible for inducing female sexual development and egg laying.

## Highlights

- *gli1* is essential for male schistosomes to induce female sexual development
- Male:female pairing induces male *Sm-nrps* expression in a *gli1*-dependent manner
- *Sm-nrps* is essential for male worms to induce female sexual development
- SmNRPS makes beta-alanyl-tryptamine, a pheromone that stimulates female development

Article

# A male-derived nonribosomal peptide pheromone controls female schistosome development

Rui Chen,<sup>1,7</sup> Jipeng Wang,<sup>1,2,3,7</sup> Irina Gradinaru,<sup>1</sup> Hieu S. Vu,<sup>4</sup> Sophie Geboers,<sup>5</sup> Jacinth Naidoo,<sup>5</sup> Joseph M. Ready,<sup>5</sup> Noelle S. Williams,<sup>5</sup> Ralph J. DeBerardinis,<sup>4,6</sup> Elliott M. Ross,<sup>1</sup> and James J. Collins III<sup>1,8,\*</sup>

<sup>1</sup>Department of Pharmacology, UT Southwestern Medical Center, Dallas, TX 75390, USA

<sup>2</sup>State Key Laboratory of Genetic Engineering, School of Life Sciences, Fudan University, Shanghai 200438, People's Republic of China

<sup>3</sup>Ministry of Education Key Laboratory of Contemporary Anthropology, School of Life Sciences, Fudan University, Shanghai 200438, People's Republic of China

<sup>4</sup>Children's Medical Center Research Institute, UT Southwestern Medical Center, Dallas, TX 75390, USA

<sup>5</sup>Department of Biochemistry, UT Southwestern Medical Center, Dallas, TX 75390, USA

<sup>6</sup>Howard Hughes Medical Institute, UT Southwestern Medical Center, Dallas, TX 75390, USA

<sup>7</sup>These authors contributed equally

<sup>8</sup>Lead contact

\*Correspondence: [jamesj.collins@utsouthwestern.edu](mailto:jamesj.collins@utsouthwestern.edu)

<https://doi.org/10.1016/j.cell.2022.03.017>

## SUMMARY

Schistosomes cause morbidity and death throughout the developing world due to the massive numbers of eggs female worms deposit into the blood of their host. Studies dating back to the 1920s show that female schistosomes rely on constant physical contact with a male worm both to become and remain sexually mature; however, the molecular details governing this process remain elusive. Here, we uncover a nonribosomal peptide synthetase that is induced in male worms upon pairing with a female and find that it is essential for the ability of male worms to stimulate female development. We demonstrate that this enzyme generates  $\beta$ -alanyl-tryptamine that is released by paired male worms. Furthermore, synthetic  $\beta$ -alanyl-tryptamine can replace male worms to stimulate female sexual development and egg laying. These data reveal that peptide-based pheromone signaling controls female schistosome sexual maturation, suggesting avenues for therapeutic intervention and uncovering a role for nonribosomal peptides as metazoan signaling molecules.

## INTRODUCTION

Schistosomes are parasitic flatworms that infect 220 million of the world's poorest people (Steinmann et al., 2006; WHO, 2018). These parasites claim more than 250,000 lives every year and cause chronic, debilitating symptoms in millions more (King, 2010; King and Dangerfield-Cha, 2008; van der Werf et al., 2003). The morbidity associated with schistosome infection is driven almost entirely by the parasite's massive egg output (Grzych et al., 1991). Indeed, these parasites can produce an egg every one to 5 min over the decades they survive in the blood (Cheever et al., 1994; Harris et al., 1984). Although the parasite's goal is to pass the eggs to the environment, many become lodged in host organs, resulting in inflammation and fibrosis that drive disease (Pearce and MacDonald, 2002). Since parasites incapable of egg production generate little pathology (Langenberg et al., 2020), strategies that blunt egg production could represent additional therapies.

In contrast to other flatworms that reproduce as hermaphrodites, schistosomes are dioecious, possessing separate male and female sexes (Cort, 1921). This sexual dimorphism was such a distinguishing characteristic that early parasitologists

created the genus *Schistosoma* to refer to the split (schistos) body (soma) of these worms (Weinland and Wyman, 1858). The male worms are large and muscular, with a specialized groove along their ventral surface, the gynecophoral canal, that the male uses to clasp the female to allow sperm transfer. Unlike the male, the female schistosome is long and slender with much of her body mass committed to egg production. Egg production in female worms relies on two large organ systems (Figure 1A, mature): the ovary, which produces oocytes, and the vitellaria, which produce vitellocytes (yolk cells) that provide egg shell constituents and nutrition for the developing embryo.

Presumably, as a consequence of hailing from hermaphroditic ancestors, male and female schistosomes have evolved several unique interactions. The most striking of these, first noted nearly a century ago, is that female sexual development is entirely governed by pairing with a male schistosome (Severinghaus, 1928). Indeed, the ovaries and vitellaria of females grown in the absence of males are present as primordia that generate no differentiated oocytes or vitellocytes (Figure 1A, immature "virgin"). As a consequence, unpaired females generate no eggs. Not only do females require males to induce their sexual development, they require perpetual coupling with a male to sustain

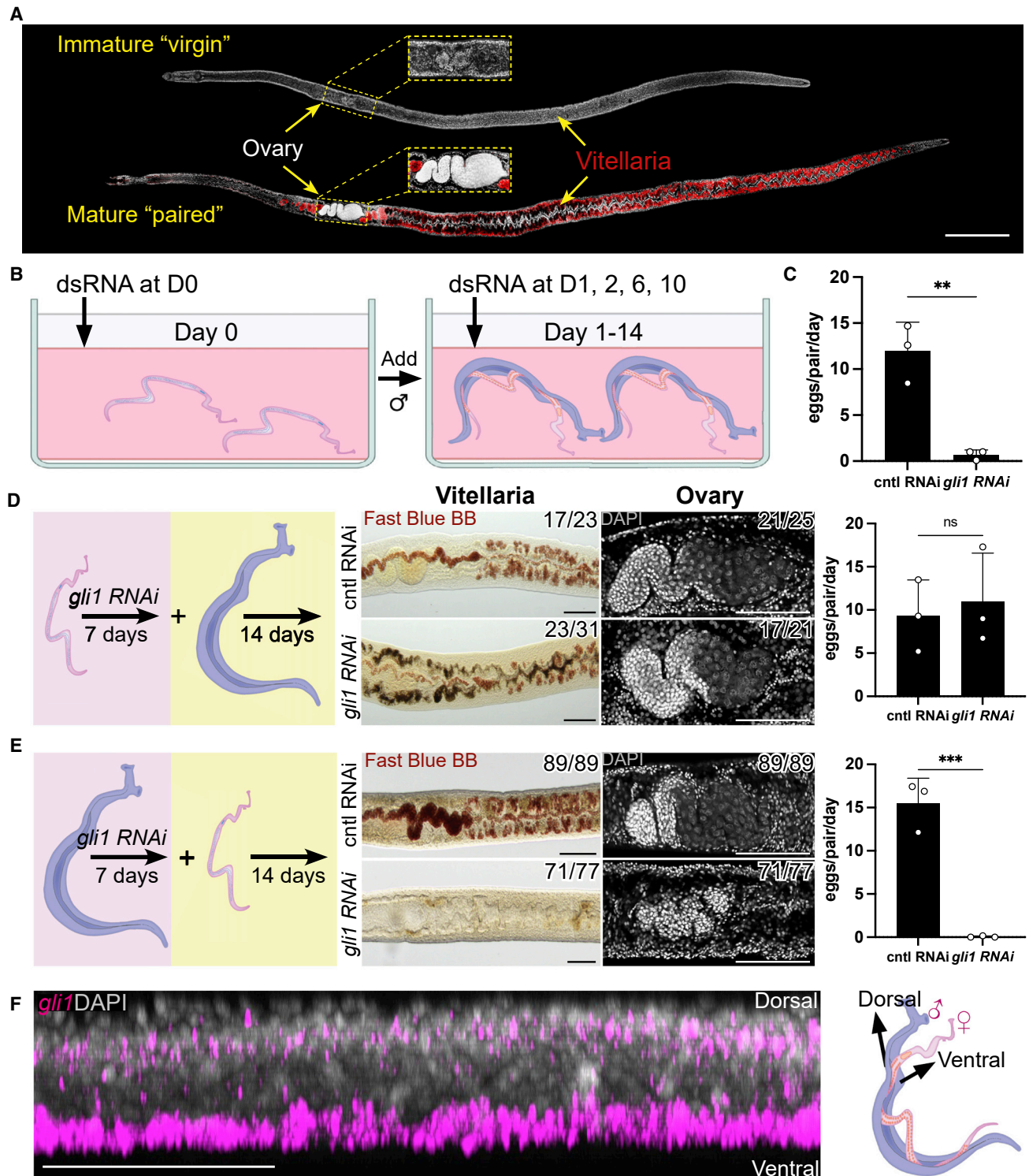


**Figure 1. *gli1* is required in male worms for female sexual development**

(A) DAPI (gray) and Fast Blue BB (red) labeling of sexually immature adult “virgin” and sexually mature “paired” adult females. Fast Blue BB labels mature vitellocytes.

(B) Schematic of the RNAi screening regime.

(C) Number of eggs laid per day per female parasite between days 12 and 14 after pairing following RNAi.  $n > 23$  worm pairs for each treatment group,  $n = 3$  biological replicates.

(legend continued on next page)

their mature reproductive status (Popiel et al., 1984). Curiously, amputated segments of male worms that lack reproductive organs can pair with virgin females and induce localized development of the female vitellaria or ovaries (Popiel and Basch, 1984; Wang et al., 2019). Thus, localized physical contact with a male, and not sperm transfer, is critical for stimulating the development of the female sexual organs. Despite progress identifying molecular pathways involved in sexual development (Greveling et al., 2018; LoVerde et al., 2009), the molecular mechanisms by which male:female pairing induces female maturation remains one of the largest outstanding mysteries in the field.

Here, we report that the expression of the transcription factor, GLI1, is critical for male schistosomes to induce female sexual development. Transcriptional profiling and biochemical studies revealed that GLI1 is essential for the induction of a nonribosomal peptide synthetase (NRPS) in male worms following pairing and that this enzyme produces a dipeptide (BATT,  $\beta$ -alanyl-tryptamine) exclusively in paired male worms. We find that paired male worms secrete BATT to the environment and that treatment of virgin females with this dipeptide can induce their development in the absence of a male worm. Together, these studies uncover a mechanism by which male schistosomes control female development.

## RESULTS

### *gli1* is required in male worms for female sexual maturation

In order to uncover genes essential for male-induced female reproductive development, we performed an RNAi screen targeting components of the major signaling pathways conserved among metazoa (Table S1). Given the broad roles for these pathways in controlling metazoan development (Perrimon et al., 2012), we reasoned that targeting one or more of these pathways could uncover molecules essential for male-stimulated female development. For this screen, we performed RNAi on virgin female worms, then on male:female worm pairs, and then measured the rate of female sexual development by monitoring egg production at D14 (Figure 1B).

From this screen, we uncovered a single gene, *gli1*, that was essential for female worms to commence egg production (Figure 1C). Since both male and female worms received *gli1* dsRNA, this effect could be due to *gli1* depletion in male and/or female worms. To distinguish between these possibilities, we performed *gli1* RNAi treatment on either virgin female parasites or male parasites for 7 days and then paired these RNAi-treated worms with untreated parasites of the opposite sex. These studies revealed that RNAi of *gli1* in female worms had no effect on the development of the vitellaria or egg production (Figure 1D). However, female worms coupled with *gli1* RNAi male worms dis-

played little vitellaria development, scant ovary differentiation, and were incapable of egg production postpairing (Figures 1E and S1A). Thus, *gli1* appears to act in male worms to control one or more processes that are critical for the stimulation of female development and egg production.

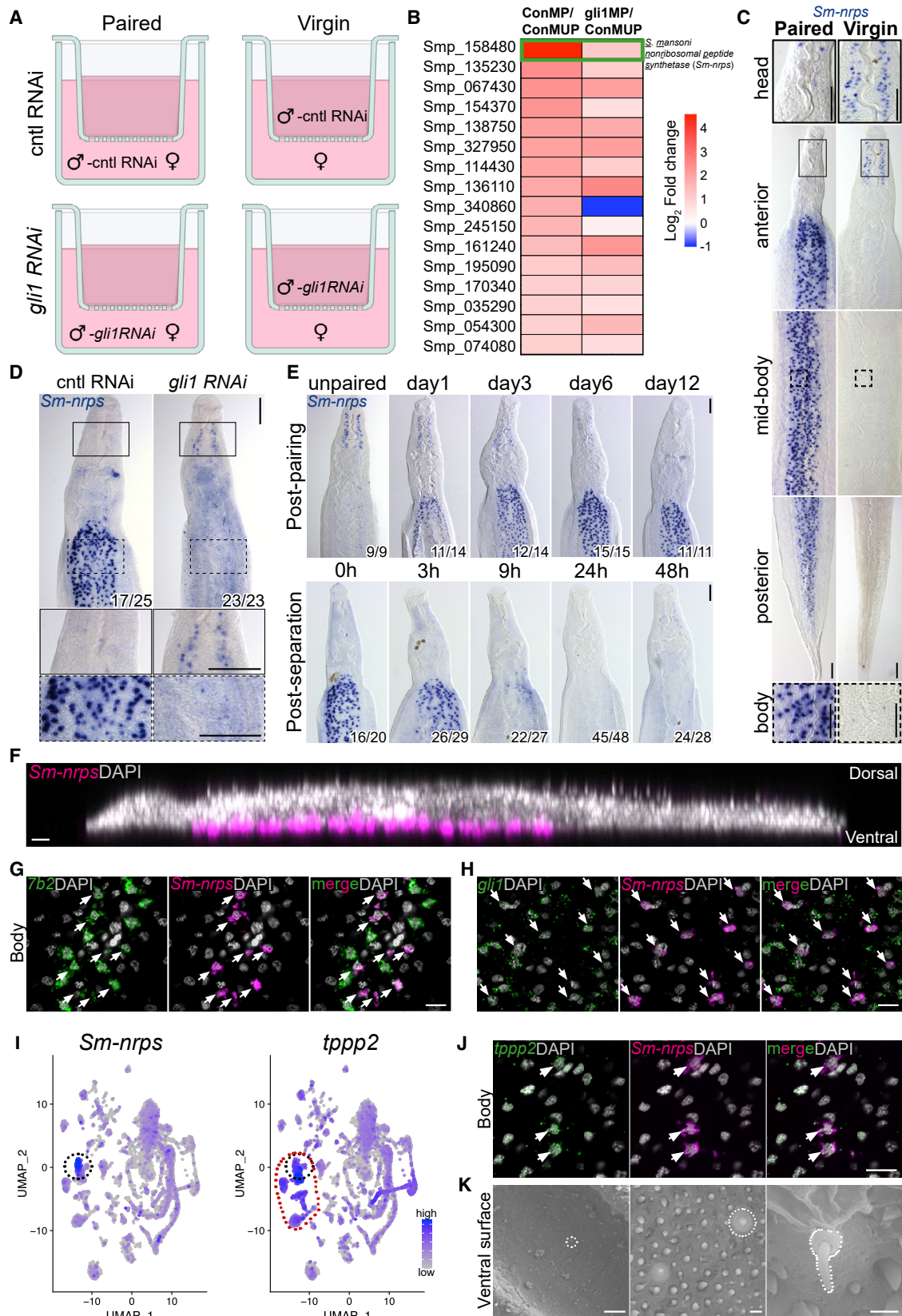
### *Sm-nrps* expression is induced in ventrally located ciliated neurons in a *gli1*-dependent manner

*gli1* is predicted to encode a zinc finger transcription factor related to the GLI family of proteins that are mediators of hedgehog-dependent and -independent signaling pathways (Pietrobono et al., 2019). Given its potential role in transcriptional regulation, we reasoned that *gli1* may control transcriptional changes in male worms that are necessary for the males to initiate processes key to induce female development. To explore this in more detail, we performed whole-mount *in situ* hybridization (WISH) to examine the distribution of *gli1* mRNA in male worms. We observed *gli1* expression in cells distributed along the ventral surface of both paired (Figure 1F) and unpaired male worms (Figures S1B and S1C; Video S1). By fluorescence *in situ* hybridization (FISH), we found that these ventrally positioned *gli1*<sup>+</sup> cells expressed markers of neurons (*7b2*, Figure S1D) and the tegument (skin) (*calpain* (*calp*), Figure S1E) in both paired and virgin males. Since the male worm contacts the female along his ventral surface, it appears that GLI1 is expressed in cells in proximity to female parasites upon pairing. Furthermore, it appears that the distribution of *gli1* mRNA is not substantially altered in male worms following pairing.

We also examined the expression of *gli1* in virgin and mature female worms. We noted *gli1* mRNA expressed bilaterally along the edges of the body in both mature and virgin females; by FISH, we found that these cells expressed the neural marker *7b2* (Figure S1G). Interestingly, we noted by WISH that mature female schistosomes expressed more *gli1* throughout their bodies (Figure S1F). By FISH, we observed that many *gli1*<sup>+</sup> cells in mature female schistosomes expressed the tegumental marker *calp* (Figure S1H). However, few *calp/gli1* double positive cells were observed in virgin females (Figure S1H). Thus, it appears that the distribution of *gli1* expression is changed in females during sexual maturation. However, since RNAi of *gli1* in females resulted in no obvious phenotypes (Figure 1D), it is challenging to speculate the significance of these observations.

To explore which genes GLI1 may control in male parasites upon pairing, we performed RNA-seq (Figure 2A). For these studies, virgin male parasites were treated with *gli1* dsRNA and either paired with virgin female worms or cocultured in wells with female worms but prohibited from pairing by a mesh cell strainer. Following 2 days of coculture, RNA from male (Figure 2B) and female worms (Figure S2A) were processed for RNA-seq. Similar to previous studies examining gene expression

(D and E) Evaluation of sexual development (center) or egg production (right) following RNAi of *gli1* in (D) female worms or (E) male worms, followed by pairing with nontreated worms of the opposite sex. Fast Blue BB (red) and DAPI (gray) staining showing the vitellaria (left) and ovary (right) from female parasites on day 14 after pairing.  $n > 21$  parasites for each treatment,  $n = 3$  biological replicates. Egg production rates were examined with  $n > 23$  worms for each treatment group. (F) Sagittal confocal section of FISH showing *gli1* (magenta) mRNA enriched in the ventral part of a male worm (left) where the male-female interaction occurs (right).  $n > 10$  parasites across 3 experiments. \*\* $p < 0.01$ ; \*\*\* $p < 0.001$ ; ns  $p > 0.05$ . Parametric t test. Error bars represent SD. Each data point represents an individual experiment. Numbers in corner indicate fraction of worms similar to those presented/total number of worms examined. Scale bars: 500  $\mu\text{m}$  in (A) and 100  $\mu\text{m}$  in (D–F).



(legend on next page)

changes in male worms upon pairing (Lu et al., 2016; Wang et al., 2017), we noted only a small group of genes (16) that were induced >2-fold in male worms postpairing (p-adj. < 0.0001, Figure 2B; Table S2). Many of these genes were not induced to the same level in the absence of *gli1* (Figure 2B). The most notable difference was in the expression of Smp\_158480, which was induced >20-fold in paired versus unpaired control males but only induced about 2-fold when *gli1* was depleted (Figure 2B). Interestingly, this gene was downregulated about 10-fold in the females after pairing, and this downregulation was also dependent on male *gli1* mRNA (Figure S2A; Table S3). These observations parallel previous studies that examined Smp\_158480 expression in paired and unpaired worms (Haerberlein et al., 2019; Lu et al., 2019). Based on BLAST, Smp\_158480 appeared to encode a NRPS similar to Ebony from *Drosophila* (Richardt et al., 2003). From here on, we will refer to Smp\_158480 as *Schistosoma mansoni nonribosomal peptide synthetase* (*Sm-nrps*).

Given the robust *gli1*-dependent induction of *Sm-nrps* expression following pairing, we conducted detailed analyses of *Sm-nrps* expression. As suggested by our RNA-seq data, WISH analysis found that *Sm-nrps* mRNA was abundantly expressed in paired male worms recovered from mixed sex infections but not in virgin male worms recovered from male-only infections (Figure 2C). *Sm-nrps* expression in paired male worms was found in distinct cells throughout the body but with expression limited to a few cells in the head (Figures 2C, left and S2B). Conversely, virgin male parasites expressed little *Sm-nrps* in their bodies but possessed bilateral “lines” of *Sm-nrps*<sup>+</sup> cells in their head. Interestingly, although paired *gli1* RNAi parasites had little expression of *Sm-nrps* in their bodies, they expressed *Sm-nrps* in their head in a manner similar to that of virgin male worms (Figures 2C and 2D). This latter result suggests that *gli1* does not simply regulate global *Sm-nrps* levels and may be required for controlling a “switch” between paired and unpaired transcriptional programs. Consistent with *Sm-nrps* expression being tightly controlled by pairing status, we observed that *Sm-nrps* mRNA levels were induced within 24 h of pairing and were rapidly depleted in male worms within 12 h of becoming divorced from their female mates (Figure 2E).

We next explored the molecular identity of the *Sm-nrps*<sup>+</sup> pairing-responsive cells in the bodies of male worms. As was

observed for *gli1*, *Sm-nrps*<sup>+</sup> cells were almost entirely found on the ventral side of male worms (Figure 2F). Examination of *Sm-nrps* expression using a single-cell RNA-seq atlas of adult schistosomes (Wendt et al., 2020) found that this gene was most highly expressed in a subpopulation of neurons (Figure 2I, left). Indeed, FISH analyses found that all *Sm-nrps*<sup>+</sup> body cells (59/59 cells examined) expressed the neural marker 7b2 (Figure 2G). As anticipated by our RNA-seq studies, these *Sm-nrps*<sup>+</sup> neurons in the body also expressed *gli1* (Figure 2H, 37/40 cells). Conversely, the small number of *Sm-nrps*<sup>+</sup> cells in the head of virgin males did not express *gli1*<sup>+</sup> (Figure S2C) and instead expressed the muscle marker *tpm2* (Figure S2D). A closer examination of the *Sm-nrps*<sup>+</sup> neuron cluster on our single-cell RNA-seq atlas and subsequent FISH studies found that these cells express *tppp2* (Figures 2I and 2J, 34/38 cells examined), a marker of ciliated cell types (Wendt et al., 2020). Since ciliated cells are often associated with sensory functions (Singla and Reiter, 2006), we reasoned that these *Sm-nrps*<sup>+</sup> neurons on the male ventral surface could represent sensory cells involved in male:female communication. The morphology of the ventral surface where the male contacts the female worm, known as the gynecophoral canal, has received little attention due to its folded structure prohibiting detailed morphological studies. Using an optimized relaxation and fixation procedure, we performed scanning electron microscopy (SEM) studies of the male ventral surface. Importantly, we observed cilium-like protrusions, roughly 1 μm in length and morphologically similar to previously described schistosome sensory cilia (Collins et al., 2011), present throughout the gynecophoral canal in both paired (Figure 2K) and unpaired male worms (Figure S2E). These data suggest that *Sm-nrps*<sup>+</sup> cells along the ventral surface are ciliated neurons potentially exposed to the environment within the gynecophoral canal.

We also analyzed the expression of *Sm-nrps* in the females by *in situ* hybridization. Consistent with our RNA-seq studies, *Sm-nrps* mRNA was most highly expressed in virgin females in cells throughout the body and was only weakly detected in sexually mature females (Figure S2F). Interestingly, the two lines of *Sm-nrps*<sup>+</sup> head cells observed in virgin males were also present in virgin female worms (Figure S2F). By FISH, we found that *Sm-nrps*<sup>+</sup> cells in both the head and body expressed the muscle marker *tpm2* but not the neural marker 7b2 (Figures S2G and S2H).

### Figure 2. RNA-seq revealed *Sm-nrps* as a *gli1*-dependent and pairing-dependent gene in male parasites

- (A) Scheme to identify *gli1*-dependent changes in gene expression following pairing. Immature females were either paired with or separated from control (cntl) or *gli1* RNAi males using a cell strainer. At 3 days of cocultivation, worms were prepared for RNA-seq.
- (B) Heatmap showing *gli1*-dependent transcriptional changes in paired male worms. ConMP, paired cntl male; ConMUP, unpaired cntl male; gli1MP, paired *gli1* RNAi male. Green rectangle highlights the *S. mansoni nonribosomal peptide synthetase* (*Sm-nrps*) gene (Smp\_158480). Genes limited to those with 2-fold change and adjusted p value < 0.0001 in the comparison of ConMP to ConMUP.
- (C and D) WISH showing the expression of (C) *Sm-nrps* mRNA in male parasites from mixed or single sex infections and (D) *Sm-nrps* following RNAi of *gli1* in paired male parasites. n > 10 parasites across 3 experiments. Insets show expression in head or body from regions enclosed in solid or dashed rectangles, respectively.
- (E) WISH showing the expression of *Sm-nrps* at various time points postpairing (top) or following separation from female worms (bottom). n = 3 experiments with n > 9 worms. For (D and E), numbers indicate fraction of worms similar to those presented/total number examined.
- (F) Sagittal confocal section of *Sm-nrps* FISH (magenta).
- (G and H) FISH showing expression of *Sm-nrps* with (G) 7b2 or (H) *gli1* in the body of paired male worms.
- (I) Single-cell sequencing UMAP plots from adult worms showing the expression of *Sm-nrps* (left) and *tppp2* (right). The black-dotted circle highlights *Sm-nrps*<sup>+</sup> cells, whereas the red-dotted circle highlights *tppp2*<sup>+</sup> ciliated neurons.
- (J) FISH for *tppp2* and *Sm-nrps* in the body of paired male worms. In (G, H, and J), arrows indicate coexpression.
- (K) Scanning electron micrographs showing the ventral surface of a male. White-dotted lines indicate a sensory cilium-like structure. Representative images from 3 parasites. In (F–H and J) nuclei are gray. Scale bars: 100 μm in (C–E), 10 μm in (F–H and J), 20 μm in (K, left), 1 μm in (K, middle), and 0.5 μm in (K, right).

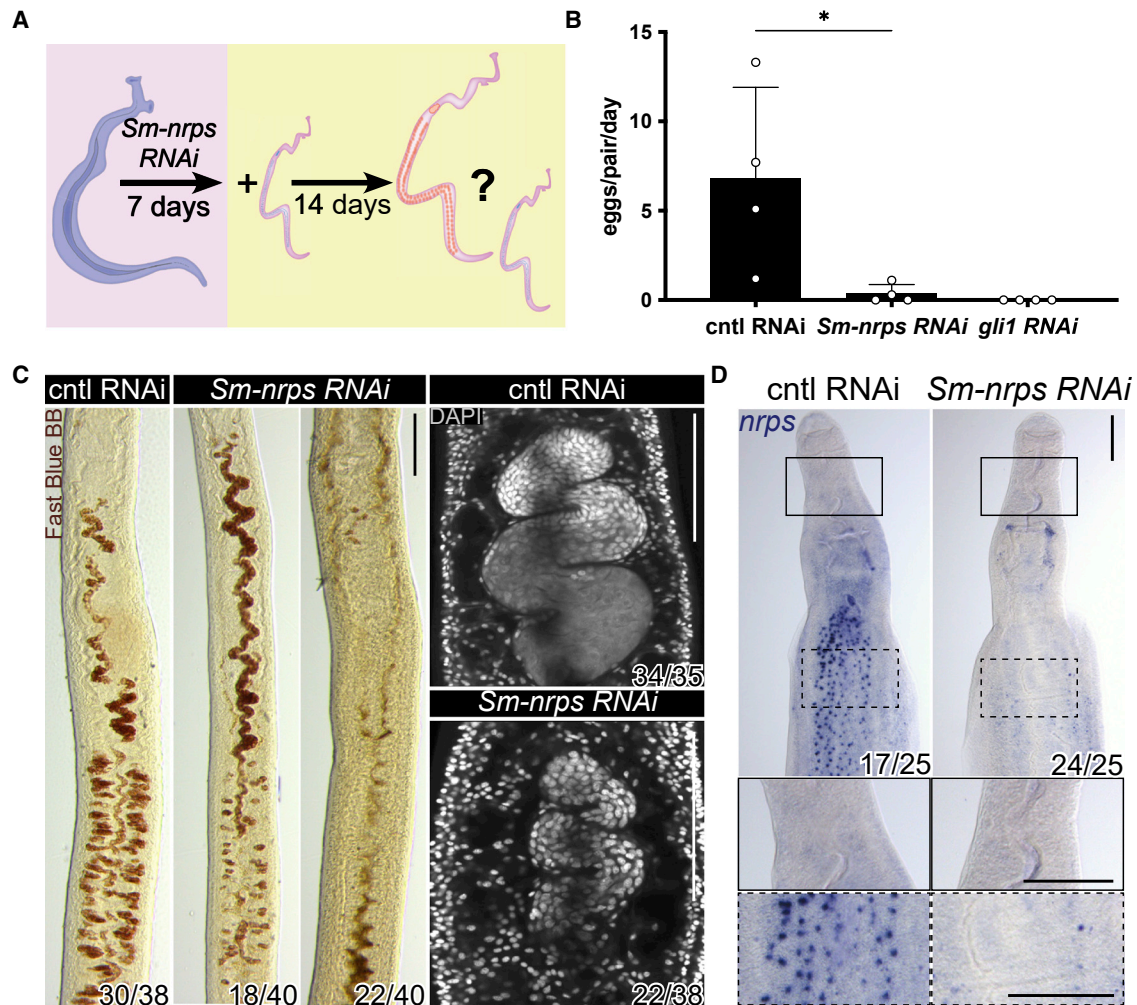


**Figure 3. *Sm-nrps* is essential in male worms for female sexual maturation**

(A) Schematic of experiments to evaluate male *Sm-nrps* in female sexual maturation.

(B) Eggs laid per day per female parasite between days 12 and 14 postpairing in *Sm-nrps* or *gli1* RNAi-treated male worms. Each data point represents an individual experiment. n > 35 parasites for each treatment group. \*p < 0.05. Parametric t test. Error bars represent SD.

(C) Fast Blue BB (red) and DAPI (gray) staining showing the vitellaria (left) and ovary (right) from female parasites D14 after pairing with *Sm-nrps* RNAi male worms. For females paired with *Sm-nrps* RNAi males, vitellaria development was either reduced (left) or absent (right). n > 3 experiments with n > 35 worms for each group.

(D) WISH for *Sm-nrps* in paired male worms following RNAi. n = 3 experiments with n > 24 worms. Numbers in corner indicate fraction of worms similar to those presented/total number examined. Scale bars: 50  $\mu$ m in (C) and 100  $\mu$ m in (D).

Unlike in paired males, *Sm-nrps* was expressed on the dorsal surface and lateral edges of the virgin female body (Figure S2I).

### ***Sm-nrps* is essential in male worms for female sexual maturation**

Motivated by our gene expression studies, we performed RNAi to evaluate the role of male *Sm-nrps* in controlling female development. For these studies, unpaired male parasites were treated with *Sm-nrps* or control dsRNA for a week and then paired with virgin females for 2 weeks (Figures 3A and S2J). Similar to what was observed with *gli1* RNAi, we found that female worms paired with *Sm-nrps* RNAi males laid ~90% fewer eggs compared with controls (Figure 3B). Female worms paired with *Sm-nrps* RNAi

males also displayed reduced Fast Blue BB staining in their vitellaria and possessed poorly developed ovaries (Figure 3C). These data support the model that *gli1*-dependent induction of *Sm-nrps* levels in male worms is critical for normal female sexual development. Unlike *gli1* RNAi males whose postpairing *Sm-nrps* expression pattern was similar to virgin parasites (Figure 2D), *Sm-nrps* RNA was not detectable in heads or bodies of *Sm-nrps* RNAi males after pairing (Figure 3D), as expected.

### **SmNRPS is a $\beta$ -alanyl-bioamine nonribosomal peptide synthetase**

NRPSs produce physiologically and clinically important secondary metabolites, including antibiotics (Süssmuth and Mainz,

2017), from standard and nonstandard amino acids. Although these enzymes are widely found in bacteria and fungi, few have been characterized outside of these taxa (Torres and Schmidt, 2019). One exception is the *D. melanogaster* Ebony protein. Ebony is composed of three domains: an N-terminal amino acid adenylation domain (A domain), a peptidyl carrier protein (PCP) or thiolation domain (T domain), and a C-terminal “amine selective” domain (Izoré et al., 2019; Richardt et al., 2003). By protein alignment with Ebony, we were able to discern both an A and a T domain in the schistosome NRPS protein sequence, suggesting this protein is potentially a true metazoan NRPS enzyme (Figures 4A and S3A).

Biochemical studies have determined that Ebony is able to conjugate  $\beta$ -alanine ( $\beta$ Ala) to a variety of biogenic amines, including serotonin, dopamine, and histamine (Hartwig et al., 2014; Richardt et al., 2003). This enzymatic process involves three steps (Figures 4B and S3B): (1) adenylation of  $\beta$ Ala catalyzed by the A domain, (2) covalent attachment of  $\beta$ Ala to a phosphopantetheinyl group on a conserved serine (ser611) within T domain, and (3) binding of an appropriate amine in the amine selective domain to facilitate nucleophilic attack of the  $\beta$ Ala group resulting in a dipeptide product. The specificity of A domain toward the first amino acid substrate can be predicted by the sequence of approximately ten residues within the substrate binding pocket of the A domain (Stachelhaus et al., 1999). Protein alignments of A domains that use  $\beta$ Ala (Ebony and the first A domain of NRPS2-1, a bacterial enzyme) and the standard reference A domain from gramicidin synthetase 1 (GS1), which uses Phe (Conti et al., 1997), found extensive similarities between SmNRPS and its homologs that use  $\beta$ Ala (Figure 4C).

To explore the ability of the schistosome enzyme to utilize  $\beta$ Ala, we purified full-length schistosome SmNRPS from insect cells (Figure S3C) and measured its amino acid-dependent ATP-PP<sub>i</sub> exchange activity (Hartwig et al., 2014; Hoagland, 1955; Richardt et al., 2003). This assay measures the ability of the enzyme to catalyze the incorporation of <sup>32</sup>P from [<sup>32</sup>P]PP<sub>i</sub> into ATP in the presence of an amino acid substrate (Figure S3D). Similar to Ebony, we found that SmNRPS was only active in the presence of  $\beta$ Ala (Figures 4D and 4E), suggesting that the SmNRPS A domain is selective for  $\beta$ Ala over other amino acids. Although SmNRPS had clear selectivity for  $\beta$ Ala, its adenylation rate in the presence of  $\beta$ Ala was roughly 8 times slower than A domain of Ebony (Figure S3E). As with Ebony (Richardt et al., 2003), the ability of SmNRPS to convert PP<sub>i</sub> to ATP was not dependent on the conserved thiolation site (Ser892) (Figure 4C, “T”) in the T domain (Figure 4F).

Next, we tested the specificity for the second amine using an “unloading assay” (Richardt et al., 2003). In this assay (Figure S3F), [<sup>3</sup>H] $\beta$ -alanine is reacted with SmNRPS to generate a [3H] $\beta$ -alanine-NRPS intermediate by the adenylation and covalent conjugation in the T domain. Then, various amines were added to the enzyme to determine whether they can displace the tritiated moiety from the enzyme. We observed that all 20 common amino acids, various monoamines/polyamines, and epinephrine possessed little activity in this assay. However, several monoamine neurotransmitters including histamine, serotonin, dopamine, and octopamine were all capable of displacing >50% of [3H] $\beta$ -alanyl moiety from the loaded enzyme (Figure 4G).

Similar to Ebony (Hartwig et al., 2014; Richardt et al., 2003), mutation of the conserved thiolation site (S892) in the T domain to alanine (S892A) reduced [<sup>3</sup>H] $\beta$ -alanine conjugation to the enzyme by ~90% (Figure 4H). These data confirm that SmNRPS is a NRPS and indicate this enzyme possesses  $\beta$ -alanyl-bioamine synthase activity *in vitro*.

### SmNRPS generates $\beta$ -alanyl-tryptamine that is secreted from paired male schistosomes

Our biochemical studies suggested that SmNRPS may conjugate  $\beta$ Ala to one or more natural monoamines *in vivo*. To determine the identity of the *in vivo* SmNRPS product, we treated paired worms with either natural  $\beta$ Ala or <sup>13</sup>C-labeled  $\beta$ Ala (Figure 5A). We then performed liquid chromatography-mass spectrometry (LC-MS) analysis on male extracts, searching for metabolites that possessed a +3-Da mass shift in extracts from the [<sup>13</sup>C3] $\beta$ Ala-labeled worms. These studies identified a metabolite (Figure 5B) corresponding to the molecular weight of BATT (Figure 5C) that was shifted +3 Da in extracts from [<sup>13</sup>C3] $\beta$ Ala labeled worms. LC-MS analysis of an unloading assay mixture with tryptamine confirmed that this ion from schistosome extracts was BATT (Figure S4A). Importantly, we did not find any evidence of [<sup>13</sup>C3] $\beta$ Ala incorporation into molecules with masses corresponding to other  $\beta$ -alanyl-bioamines (e.g.,  $\beta$ -alanyl-dopamine, -histamine, -serotonin, etc.) that SmNRPS generates *in vitro* (Figure 4G). The incorporation of [<sup>13</sup>C3] $\beta$ Ala into BATT was only observed in male parasites (Figure 5D), and this ion was not observed in extracts from paired female worms (Figure S4B). To determine if the production of BATT in male worms was dependent on *Sm-nrps* expression, we performed RNAi studies along with LC-MS analyses (Figure 5E). We found that RNAi of either *gli1* or *Sm-nrps* blocked the ability of worms to incorporate [<sup>13</sup>C3] $\beta$ Ala into BATT by >90% (Figure 5F) and abolished total BATT levels (Figure S4C). Taken together, our data suggest BATT to be the physiologically relevant product of SmNRPS in male worms.

Using chemically synthesized BATT as a standard, we next quantified naturally occurring BATT levels in paired and unpaired male worms. As suggested by the expression of *Sm-nrps* (Figure 2C), we only detected high levels of BATT in samples from paired male worms (Figure 5G). In principle, BATT could act either as an endogenous factor in males required for them to promote female development or BATT could be released from male worms to act directly on females. To explore these possibilities, we cultured paired male worms or isolated male or female worms and quantified BATT levels in media after 48 h of culture. BATT was not detected in media conditioned by virgin male, virgin female, or male worms that had been separated from females 3 days prior to the experiment (Figure 5H). In contrast, media conditioned by males continuously paired with female worms contained an average of 16.6 ng/mL (71 nM) BATT (Figure 5H). Interestingly, male worms separated from females on day 0 of the experiment released ~70% less BATT into the media than males that remained continuously paired (Figure 5H), indicating that, like *Sm-nrps* expression (Figure 2E), BATT production drops rapidly in the absence of female worms. In summary, our data suggest that SmNRPS induction upon pairing results in the production of BATT, and this molecule is released from the male worm into the environment.

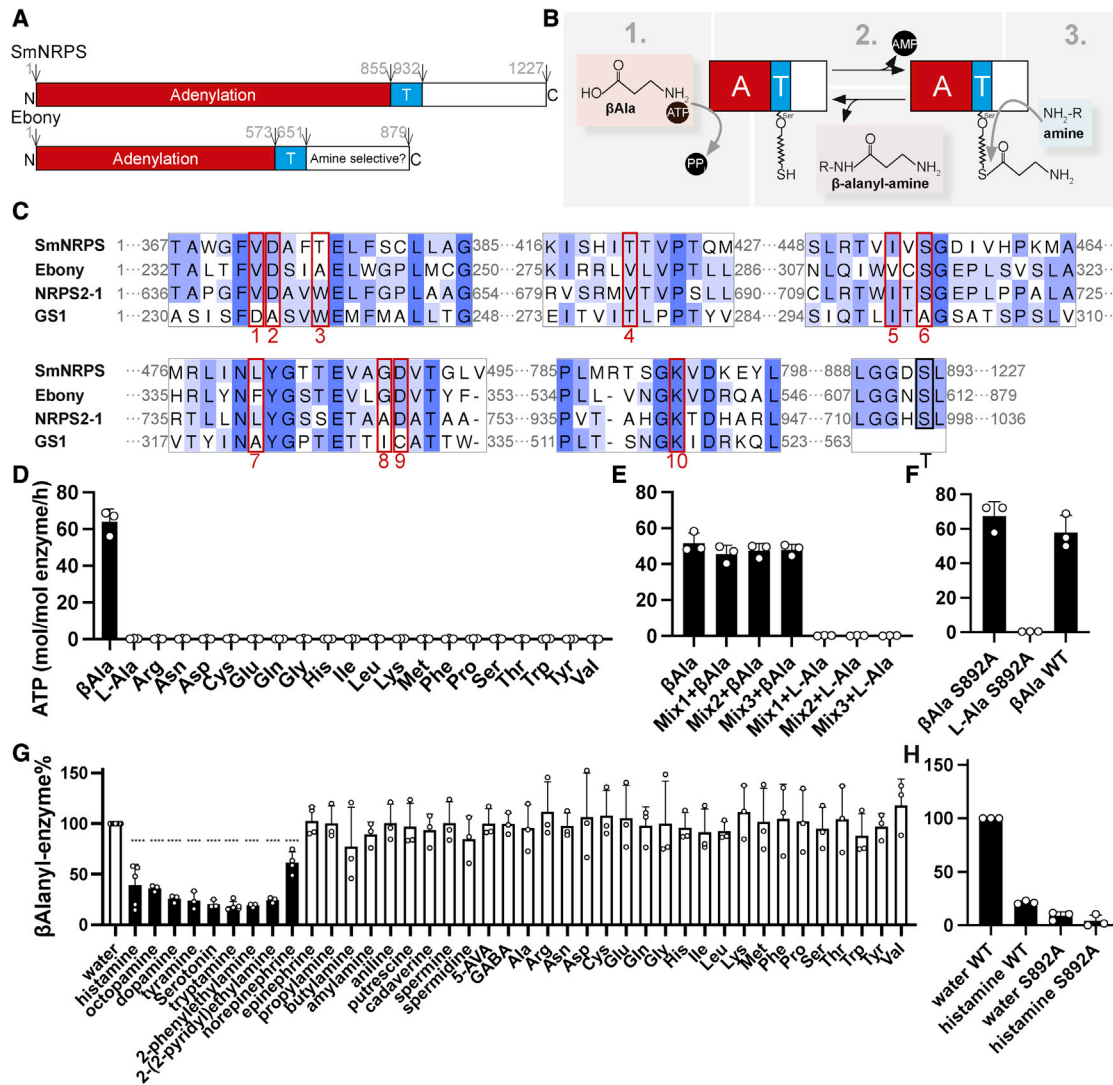


**Figure 4. SmNRPS functions as a  $\beta$ -alanyl-bioamine nonribosomal dipeptide synthetase *in vitro***

(A) Diagram showing predicted domains of SmNRPS and Ebony.

(B) Schematic showing Ebony enzymology. Details see Figure S3B.

(C) MUSCLE protein alignment of A and T domain regions from SmNRPS and two related enzymes. 10 amino acids boxed in red represent residues involved in  $\beta$ Ala selectivity in Ebony and the first A domain of NRPS2-1 from *Streptomyces verticillus* (UniProt: Q9FB18) and Phe selectivity in gramicidin synthetase 1 (GS1) (PDB: 1AMU) from *Brevibacillus brevis*. The conserved serine thiolation site in the T domain is shown by a black rectangle.

(D) ATP-PP<sub>i</sub> exchange assay showing the activity of SmNRPS with  $\beta$ Ala and the standard 20 amino acids.

(E) ATP-PP<sub>i</sub> exchange assay showing the activity of SmNRPS with pools of amino acids  $\pm$   $\beta$ Ala. Mix1: A, R, N, C, Q, G, H, and I; Mix2, L, K, M, F, P, S, T, and V; and Mix3, D, E, W, and Y.

(F) ATP-PP<sub>i</sub> exchange assay with thiolation-deficient mutant SmNRPS(S892A) with  $\beta$ Ala as a substrate. (D–F) share the same y axis title.

(G) Unloading assay with <sup>3</sup>H- $\beta$ Ala evaluating various amines as secondary substrates. Monoamine neurotransmitters and norepinephrine (black bars) drove significant  $\beta$ -alanyl unloading from SmNRPS. \*\*\*\*p < 0.0001. Parametric t test.

(H) Unloading assay with thiolation-deficient SmNRPS(S892A) mutant compared with wild-type enzyme. (G and H) share the same y axis title. All values graphed in the unloading assays were normalized to a wild-type water control within the same experiment. Each data point is the average of two technical replicates from an individual experiment. Error bars represent SD.

### BATT is sufficient to induce egg laying in virgin female parasites

The secretion of BATT from male worms suggested that BATT may act to directly stimulate female development. To examine this possibility, we first evaluated the effects of low concentra-

tion BATT on female gene expression after short-term treatment. Our previous RNA-seq studies (Figure S2; Table S3) identified genes upregulated and downregulated in female worms post-pairing whose regulation was dependent on *gli1* function in male worms. We selected two such genes for analysis: a *rotund*

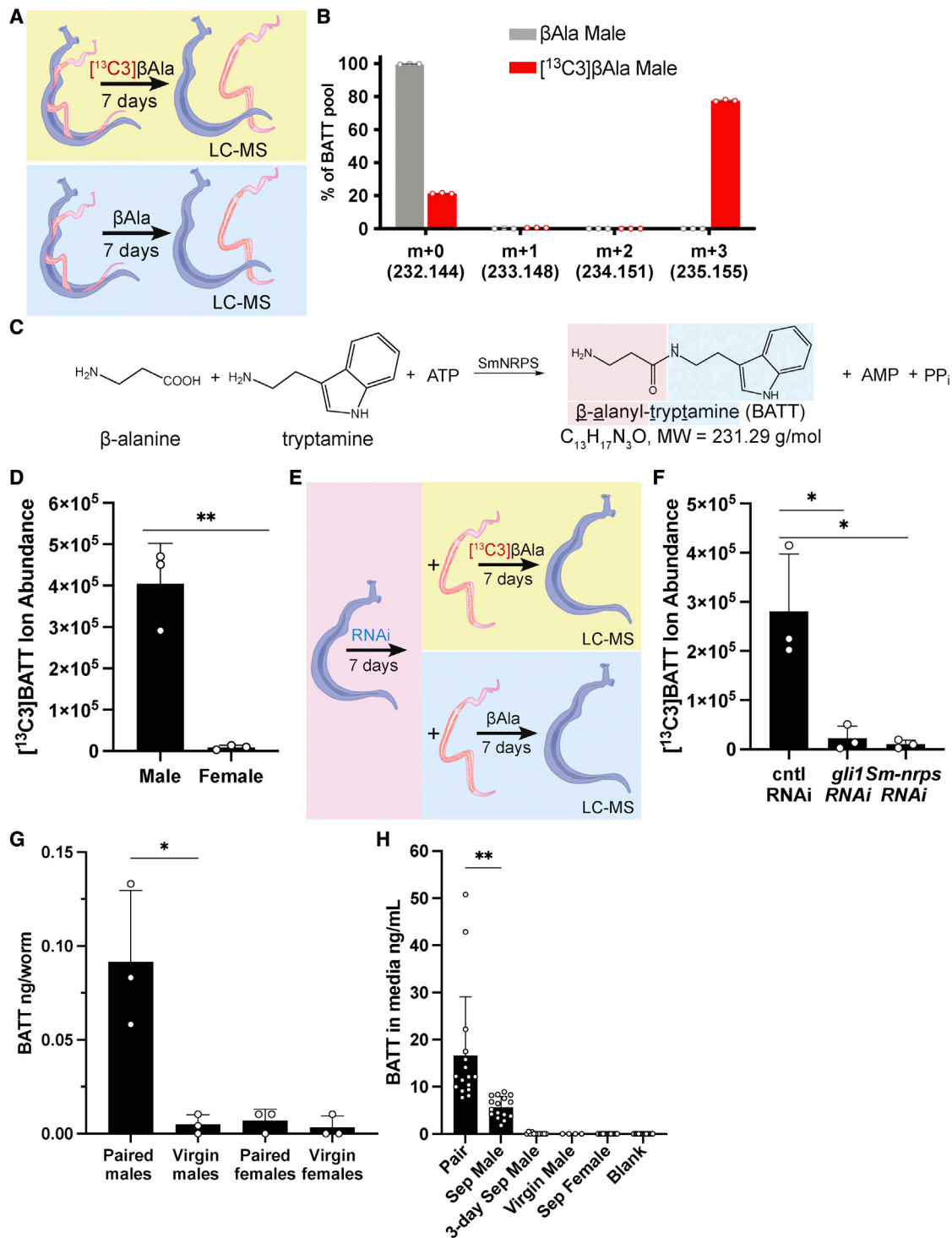


**Figure 5. SmNRPS produces  $\beta$ -alanyl-tryptamine (BATT) in paired male parasites in a *gli1*-dependent fashion**

(A) A schematic diagram showing strategy to uncover SmNRPS products utilizing  $[^{13}\text{C}_3]\beta\text{Ala}$ .

(B) Plot showing relative abundance of ions in paired male parasites treated with standard (gray) or  $[^{13}\text{C}_3]$  (red)  $\beta\text{Ala}$ . n = 3 biological replicates.

(C) Chemical structure and formula of  $\beta$ -alanyl-tryptamine (BATT) and its potential synthesis by SmNRPS.

(D) Abundance of  $[^{13}\text{C}_3]\text{BATT}$  in paired males and female parasites 7 days after  $[^{13}\text{C}_3]\beta\text{Ala}$  treatment.

(E) Regimen for evaluating effects of RNAi on  $[^{13}\text{C}_3]\text{BATT}$  production.

(F) Abundance of  $[^{13}\text{C}_3]\text{BATT}$  in *gli1* or *Sm-nrps* RNAi paired male worms following 7D of  $[^{13}\text{C}_3]\beta\text{Ala}$  treatment.

(legend continued on next page)

(Smp\_169260) homolog that was induced in females only when paired with *gli1*<sup>+</sup> males and *Sm-nrps* that was downregulated in females postpairing with *gli1*<sup>+</sup> males (Figure 6A). Treatment of separated females for 24 h with 0.5  $\mu$ M synthetic BATT induced both a significant decrease in *Sm-nrps* mRNA and an increase in *rotund* mRNA (Figure 6B) when compared with controls treated with  $\beta$ Ala alone. The magnitude of the transcriptional changes of *Sm-nrps* and *rotund* following BATT treatment were comparable in magnitude with those resulting from pairing with male worms (Figures 6A and 6B).

Encouraged by the gene expression changes induced by BATT, we evaluated its effects on virgin female development. Strikingly, virgin female schistosomes commenced egg production with  $\geq 0.5 \mu$ M BATT as early as 4 days after initial treatment (Figures 6C and 6D). No egg production was observed with  $\beta$ Ala treatment or 50 nM BATT (Figure 6C). This latter result is consistent with the observation that conditioned media that contained  $\sim 70$  nM BATT also failed to induce sexual development (Figure S4D). Examination of virgin females treated with  $\geq 0.5 \mu$ M BATT found that they produced mature Fast Blue BB<sup>+</sup> vitellogocytes and possessed ovaries that contained mature oocytes (Figures 6E, S5A, and S5B). Indeed, examination of the expression of the vitellogocyte-specific marker *p48* and the oocyte-specific marker *bmpg* confirmed that BATT treatment induces maturation of the female reproductive machinery (Figure S5C). We observed similar female stimulatory activity using two batches of synthetic BATT (mcBATT and swBATT), confirming the specificity of this effect (Figures 6C, S5A, and S6B). The rate of egg production following BATT treatment was lower than that induced by male:female pairing (Figure 6C), and only about 16% of BATT-treated females contained *bmpg*<sup>+</sup> ovaries despite visible ovary differentiation (Figure S5C). These differences may indicate either that some feature of pairing is required for the complete egg laying phenomenon in addition to BATT or, alternatively, that a simple addition of BATT to the medium is not as effective as localized delivery.

To further evaluate the effects of BATT on female development, we performed RNA-seq analyses comparing virgin females at D8 following treatment with 5  $\mu$ M BATT or  $\beta$ Ala (Table S4). We then selected the 89 most differentially regulated genes ( $\log_2$  fold change  $\pm 2$ , adjusted  $p < 0.05$ ) following BATT treatment and evaluated how these genes were regulated in virgin versus sexually mature worms using a previously collected dataset (see key resources table). Remarkably, of the 87 of 89 genes that were upregulated or downregulated following BATT treatment were similarly regulated in sexually mature versus virgin worms (Figures 6F and S6A). We next queried where these 89 BATT-regulated genes were expressed on our single-cell RNA-seq atlas (Wendt et al., 2020). Consistent with BATT stimulating development of the sexual organs, roughly 60% of BATT-regulated genes were most highly expressed in cell clusters associated with late stages of development of the ovary and vitellaria

(“late female germ cells” and “differentiated vitellaria,” Figure S6B). Taken together, these data highlight that BATT induces molecular changes associated with female sexual development.

BATT treatment elicited egg production in virgin female worms several days faster than pairing with virgin male worms (Figure 6D), suggesting that it may take several days before virgin male worms can produce sufficient quantities of BATT to stimulate female development. Previous studies have shown that *in vitro* pairing with castrated male worm segments can induce virgin females to lay eggs that contain parthenogenic embryos capable of limited development (Wang et al., 2019). Examination of the eggs produced by BATT-treated virgin females found that these eggs (Figure 6G) possessed a lateral spine characteristic of *S. mansoni* eggs (Figure S5D) and that a small fraction of these eggs ( $\sim 5\%$ ) contained clusters of proliferative EdU<sup>+</sup> embryonic cells (Figure 6H). Together, these data support the model that BATT can replace a male partner to trigger egg production.

## DISCUSSION

The data presented here indicate that male:female pairing induces the GLI1-dependent expression of *Sm-nrps* in male worms, resulting in the production of BATT. BATT is then released from the male to act as a pheromone that stimulates female sexual development (Figure 7). This implies that males first “sense” the presence of the female to commence BATT production and that females possess the necessary signaling machinery to interpret the presence of BATT.

Pairing with amputated male worm segments induces development of female reproductive organs only in regions in direct contact with the male worm (Popiel and Basch, 1984; Wang et al., 2019). So, if BATT is diffusible into the medium (Figure 5H), why does it not stimulate the development of regions not in contact with male worms? We find that single paired male worms can condition media with BATT to a concentration of  $\sim 70$  nM over 48 h and that this conditioned media cannot induce virgin female sexual maturity (Figure S4D). Similar concentrations of synthetic BATT are also not sufficient to stimulate virgin female development (Figures 6C, S5A, and S5B). Since the volume of the gynecophoral canal, where males probably release BATT, is much smaller than the total culture volumes for these experiments, the local BATT concentrations female experience while paired are probably in the micromolar range in which BATT induces development.

Ciliated neurons play numerous roles in sensory perception in animals (Singla and Reiter, 2006). Thus, the expression of *Sm-nrps* in ciliated neurons on the male’s ventral surface suggests the possibility that these cells are critical for detecting the presence of the female and in turn stimulating BATT production. Interestingly, studies in *C. elegans* have demonstrated that ciliated sensory neurons can release material into the environment enclosed in exosome-like vesicles (Wang et al., 2014b). This

(G) Measurement of BATT in extracts from virgin or 14-day paired virgin (paired) male/female parasites. For (C, F, and G), each dot is an individual biological replicate derived from extracts from 30 parasites.

(H) BATT quantity in media conditioned by parasites for 2 days. “Sep Male” and “Sep Female” represents media from parasites unpaired at the beginning of the experiment. “3-day Sep Male” represents media from males separated from females 3D prior to experiment. Each dot represents the BATT concentration in media conditioned from an individual worm or worm pair. \*\* $p < 0.01$ , \* $p < 0.05$ . Parametric t test. Error bars are SD.

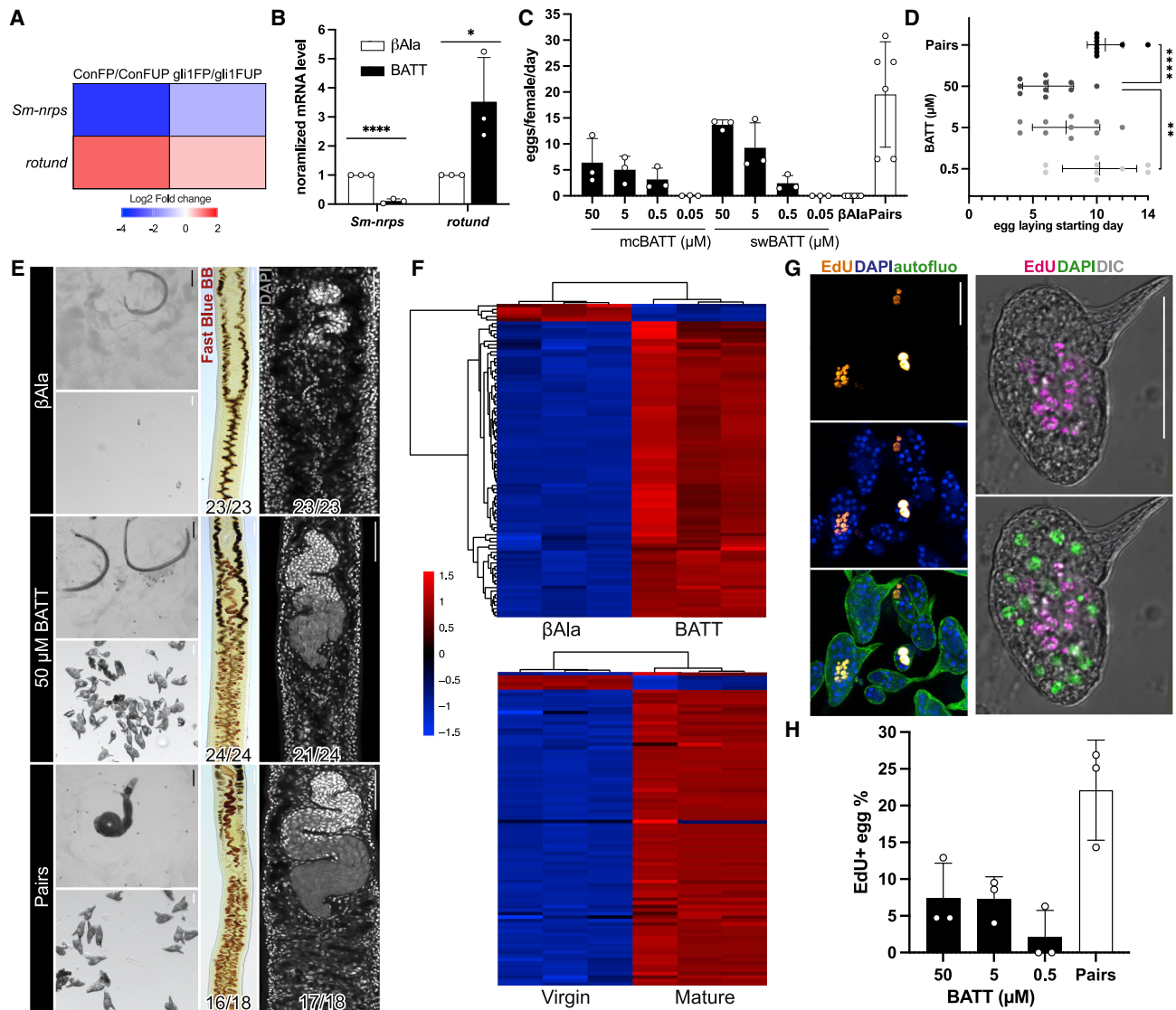


**Figure 6. Synthetic  $\beta$ -alanyl-tryptamine (BATT) is sufficient to induce egg laying in virgin female parasites**

(A) Heatmap expression of *Sm-nrps* and *rotund* mRNA levels in female parasites following pairing with control or *gli1 RNAi* parasites described in Figure 2A. (B) qRT-PCR showing relative expression of *Sm-nrps* and *rotund* following treatment of unpaired female worms with 0.5  $\mu\text{M}$  BATT for 1 day. \*\*\*\*p < 0.0001, \*p < 0.05. t test. n = 3 biological replicates. (C) Eggs laid per day per female parasite between days 12 and 14 following treatment with two sources of synthetic BATT (mcBATT or swBATT) or  $\beta\text{Ala}$  treatment or following pairing with male worms. n > 45 females for each treatment group; n > 10 for the paired group. (D) Time course of egg production following treatment with three increasing concentrations of BATT (y axis) or following pairing. \*\*\*\*p < 0.0001, \*\*p < 0.01. Parametric t test. (E) Images of worms (top left), eggs (bottom left), Fast Blue BB (middle), and DAPI (right) staining 14 days after exposure of virgin females to  $\beta\text{Ala}$ , 50  $\mu\text{M}$  BATT, or to pairing. Representative images from 3 experiments with n > 23 worms for chemical treatment group and n > 10 for paired group. Numbers in corner indicate fraction of worms similar to those presented/total number of worms examined. (F) Top, clustered heatmap of 89 differentially expressed genes following 8D of 5  $\mu\text{M}$  BATT treatment. Bottom, heatmap showing expression of same 89 genes in virgin versus sexually mature female *S. mansoni*. (G) (Left) EdU labeling (gold) of proliferative embryonic cells within the eggs laid by virgin females treated with 50  $\mu\text{M}$  BATT. Autofluorescence (autofluo, green) and DAPI (blue) shows the eggshell and nuclei, respectively. (right) Confocal image of EdU-labeled (magenta) egg laid by a virgin female treated with 50  $\mu\text{M}$  BATT. DAPI, green. DIC, differential interference contrast. (H) Percentages of EdU+ eggs laid by virgin female parasites between days 12 and 14 after BATT treatment or pairing. n > 250 eggs. In plots, each dot represents an individual experiment and error bars represent SD. Scale bars, 500  $\mu\text{m}$  (black); scale bars, 50  $\mu\text{m}$  (white).

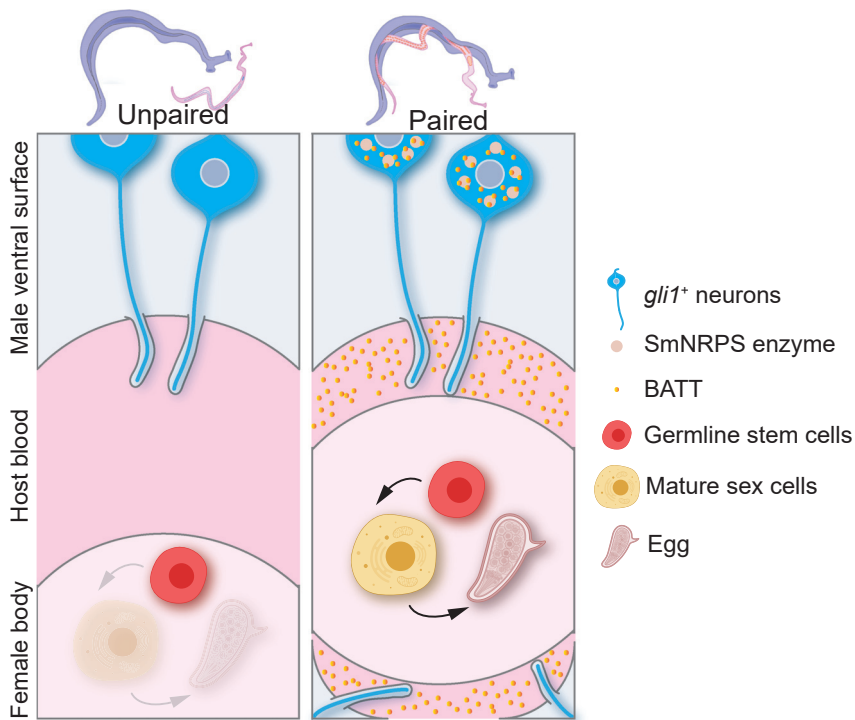


**Figure 7. Model for BATT-mediated regulation of female development from male pheromone secretion**

In the absence of the female, *gli1*<sup>+</sup> ciliated neurons protrude into the gynecophoral canal and express little SmNRPS, and BATT is not produced. When females are present, males sense the presence of the female, perhaps via *gli1*<sup>+</sup> ciliated neurons, inducing the expression of SmNRPS and BATT synthesis. Synthesized BATT is then released at concentrations sufficient to induce female sexual development accumulate in the gynecophoral canal.

observation, along with the fact adult schistosomes produce exosome-like vesicles (Sotillo et al., 2016) and that vesicles have been observed in adult schistosome sensory cilia (Hockley, 1973; Morris and Threadgold, 1967), suggests that *Sm-nrps*<sup>+</sup> neurons could be responsible not only for the perception of the female but also for the release of BATT into the environment.

NRPS enzymes are widely found in bacteria and fungi where they produce secondary metabolites that can act as toxins, pigments, siderophores, and antibiotics (Süssmuth and Mainz, 2017). However, relatively few NRPS enzymes have been characterized in animals (Shou et al., 2016; Torres and Schmidt, 2019; Wang et al., 2014a), and thus, their potential roles in metazoan biology remains largely unexplored. Perhaps, the best characterized metazoan NRPS enzyme is Ebony, which is critical for *Drosophila* cuticle pigmentation (Wright, 1987) and neurotransmission (Borycz et al., 2002). Unlike NRPS enzymes in bacteria and fungi, Ebony is not thought to produce any biologically active molecules but rather inactivate them. For instance, histamine is a key neurotransmitter in the visual system and is deactivated and recycled by its conversion to  $\beta$ -alanyl-histamine (carcinine) by Ebony in glial cells (Borycz et al., 2012; Stenesen et al., 2015; Ziegler et al., 2013). In contrast to flies, our data suggest that the SmNRPS product BATT directly stimulates signaling in the female, culminating in female development. Since BATT has not previously been recognized as a signaling molecule, the nature of the signaling pathway(s) that mediates its effect, and whether they are related to pathways characterized in other metazoa, remains unclear.

Interestingly, genes for SmNRPS-like proteins with A domains potentially selective for  $\beta$ -alanine are found not only in insects and in all schistosome species that infect humans but also in

the genomes of free-living and parasitic flatworms, rotifers, annelids, cnidarians, and at least one hemichordate (Figure S7; Table S5). Thus, BATT-like molecules may participate in cellular signaling in diverse invertebrate organisms to regulate diverse processes. Because schistosomes are the only major group of dioecious flatworms, the presence of SmNRPS in hermaphroditic flatworms is intriguing. Should SmNRPS enzymes in hermaphroditic flatworms produce BATT-like molecules necessary for development of the female reproductive system, it would suggest that, during the transition from hermaphroditism to dioecy, SmNRPS product formation was “outsourced” to the male where it could act as a pheromone, rather than an endogenous hormone, to dictate the timing of female development. Clearly, exploring SmNRPS function not just in flatworms but in a variety of metazoa may uncover more paradigms for cell-to-cell, or even animal-to-animal, communication.

BATT is capable of inducing egg production in virgin females days before females paired with virgin males (Figure 6D) and inducing transcriptional changes associated with sexual development (Figure 6F). However, the rate of egg production, the quality of eggs, and the sexual development induced by BATT (especially with the ovary) were inferior to those induced by intact male worms (Figures 6C, S5A, and S5B). Thus, BATT may act in parallel with other factors to support robust female development. One possible explanation is that BATT is a key signal to initiate development; however, the male worms provide additional factors key for optimal development. Indeed, radiolabeling studies have suggested that male worms transfer molecules such as glucose (Conford and Huot, 1981) and cholesterol (Haseeb et al., 1985; Popiel and Basch, 1986) to female worms. Also, since immune signals are important for optimal female development (Davies et al., 2001), there may be host factors that potentiate the response to BATT. Alternatively, females may perceive pairing with a male and alter their behavior or metabolism in a BATT-independent manner. However, another possibility is that BATT is packaged (for instance, in vesicles or with a cofactor) and delivered from males in a manner optimal for female BATT recognition or absorption. Clearly, more detailed assessments of the similarities between paired females and those

treated with BATT will provide additional insights into the mechanisms that ensure robust female development.

Nearly a century ago, Aura Severinghaus detailed the role of the male schistosome in female development and offered that “it is conceivable that hormones produced by the male may in some way be connected to the phenomenon” (Severinghaus, 1928). Our studies identify BATT as a male-derived pheromone that stimulates sexual development in female schistosomes. These observations provide key insights into one of the longest-standing mysteries in schistosome biology and suggest that therapeutically blocking BATT signaling could present an opportunity to blunt both schistosome transmission and egg-induced pathology. SmNRPS is a clear target, but the identification of BATT also permits study of its receptor and downstream signaling in females. Studies of this pathway both in schistosomes and other metazoa may elucidate additional cellular signaling mechanisms as well as targets for therapeutic intervention.

### Limitations of the study

BATT is a pheromone released from males that induces female *S. mansoni* sexual development. However, important questions remain. First, it is unclear how BATT is released from male worms and how and where it acts on female worms. Our data suggest that SmNRPS is expressed in ciliated neurons present on the ventral side of male and that sensory cilia are present on the male ventral surface, but technical limitations have prohibited our ability to definitively show these ventral sensory cells are the source of BATT for release. Second, our work has only focused on a single species of schistosome; hence, it is not clear how generalizable our results are to other species. However, studies in *S. japonicum* have shown that NRPS is induced in males upon coupling with a female (Lu et al., 2019; Wang et al., 2017). Also, studies have shown that males of one schistosome species can induce the sexual development of females of another (Armstrong, 1965). Taken together, it is reasonable to assume that the effects of BATT are generalizable. However, given the promiscuity of SmNRPS for various monoamines (Figure 4G), it remains possible that some schistosome species, of which there are hundreds that infect mammals and birds, generate species-specific BATT-like molecules. This could be a strategy in regions endemic to multiple species to ensure sexual reproduction only occurs with mates capable of producing viable offspring.

### STAR★METHODS

Detailed methods are provided in the online version of this paper and include the following:

- KEY RESOURCES TABLE
- RESOURCE AVAILABILITY
  - Lead contact
  - Materials availability
  - Data and code availability
- EXPERIMENTAL MODEL AND SUBJECT DETAILS
  - *S. mansoni* parasites
  - *S. mansoni* infected mice

- *B. glabrata* snails
- METHOD DETAILS
  - RNA interference (RNAi)
  - Parasite/egg staining and imaging
  - Gene expression analyses
  - Scanning electron microscopy (SEM)
  - Protein expression and purification
  - Biochemical analysis of SmNRPS
  - Metabolomic analysis
  - BATT detection in conditioned media
  - BATT synthesis and treatment
- QUANTIFICATION AND STATISTICAL ANALYSIS

### SUPPLEMENTAL INFORMATION

Supplemental information can be found online at <https://doi.org/10.1016/j.cell.2022.03.017>.

### ACKNOWLEDGMENTS

We thank members from Collins lab, Phillip A. Newmark, and Melanie H. Cobb for comments on the manuscript; the NIAID Schistosomiasis Resource Center of the Biomedical Research Institute (Rockville, MD) for providing infected snails and infected mice through NIH-NIAID contract HHSN2722017000141 for distribution through BEI Resources; Helmut Krämer for providing Ebony cDNA; the UT Southwestern Electron Microscopy and Genomics Core Facilities; and Francisco Ortiz from Preclinical Pharmacology Core Lab. Biorender was used for some schematic material. This work was funded by NIH grants R01AI121037 (J.J.C.), R01AI150776 (J.J.C.), and R35CA22044901 (R.J.D.); Welch Foundation grant I-1948-20180324 (J.J.C.); and the Burroughs Wellcome Fund (J.J.C.). R.J.D. is an HHMI investigator.

### AUTHOR CONTRIBUTIONS

Conceptualization, R.C., J.W., and J.J.C.; methodology, R.C., J.W., E.M.R., and J.J.C.; formal analysis, J.J.C.; investigation, R.C., J.W., I.G., H.S.V., and S.G.; resources, J.N. and J.M.R.; writing – original draft, R.C. and J.J.C.; writing – review & editing, R.C., E.M.R., and J.J.C.; visualization, R.C. and J.J.C.; supervision, J.M.R., N.S.W., R.J.D., E.M.R., and J.J.C.; project administration, R.C., J.W., and J.J.C.; funding acquisition, J.J.C. and R.J.D.

### DECLARATION OF INTERESTS

R.J.D. is on the SABs for Agios Pharmaceuticals, Vida Ventures, and Nirogyone Therapeutics and is a founder/advisor for Atavistik Biosciences.

Received: October 19, 2021

Revised: January 18, 2022

Accepted: March 11, 2022

Published: April 5, 2022

### REFERENCES

- Armstrong, J.C. (1965). Mating behavior and development of schistosomes in the mouse. *J. Parasitol.* 51, 605–616.
- Basch, P.F. (1981). Cultivation of *Schistosoma mansoni* in vitro. I. Establishment of cultures from cercariae and development until pairing. *J. Parasitol.* 67, 179–185.
- Borycz, J., Borycz, J.A., Edwards, T.N., Boulianne, G.L., and Meinertzhagen, I.A. (2012). The metabolism of histamine in the *Drosophila* optic lobe involves an ommatidial pathway:  $\beta$ -alanine recycles through the retina. *J. Exp. Biol.* 215, 1399–1411.

- Borycz, J., Borycz, J.A., Loubani, M., and Meinertzhagen, I.A. (2002). tan and ebony genes regulate a novel pathway for transmitter metabolism at fly photoreceptor terminals. *J. Neurosci.* *22*, 10549–10557.
- Cheever, A.W., Macedonia, J.G., Mosimann, J.E., and Cheever, E.A. (1994). Kinetics of egg production and egg excretion by *Schistosoma mansoni* and *S. japonicum* in mice infected with a single pair of worms. *Am. J. Trop. Med. Hyg.* *50*, 281–295.
- Collins, J.J., Hou, X., Romanova, E.V., Lambrus, B.G., Miller, C.M., Saberi, A., Sweedler, J.V., and Newmark, P.A. (2010). Genome-wide analyses reveal a role for peptide hormones in planarian germline development. *PLoS Biol.* *8*, e1000509.
- Collins, J.J., III, King, R.S., Cogswell, A., Williams, D.L., and Newmark, P.A. (2011). An atlas for *Schistosoma mansoni* organs and life-cycle stages using cell type-specific markers and confocal microscopy. *PLoS Negl. Trop. Dis.* *5*, e1009.
- Collins, J.J., Wang, B., Lambrus, B.G., Tharp, M.E., Iyer, H., and Newmark, P.A. (2013). Adult somatic stem cells in the human parasite *Schistosoma mansoni*. *Nature* *494*, 476–479.
- Conford, E.M., and Huot, M.E. (1981). Glucose transfer from male to female schistosomes. *Science* *213*, 1269–1271.
- Conti, E., Stachelhaus, T., Marahiel, M.A., and Brick, P. (1997). Structural basis for the activation of phenylalanine in the non-ribosomal biosynthesis of gramicidin S. *EMBO J.* *16*, 4174–4183.
- Cort, W.W. (1921). Sex in the trematode family Schistosomidae. *Science* *53*, 226–228.
- Davies, S.J., Grogan, J.L., Blank, R.B., Lim, K.C., Locksley, R.M., and McKerrow, J.H. (2001). Modulation of blood fluke development in the liver by hepatic CD4<sup>+</sup> lymphocytes. *Science* *294*, 1358–1361.
- Dobin, A., Davis, C.A., Schlesinger, F., Drenkow, J., Zaleski, C., Jha, S., Batut, P., Chaisson, M., and Gingeras, T.R. (2013). STAR: ultrafast universal RNA-seq aligner. *Bioinformatics* *29*, 15–21.
- Grevelding, C.G., Langner, S., and Dissous, C. (2018). Kinases: molecular stage directors for schistosome development and differentiation. *Trends Parasitol.* *34*, 246–260.
- Grzych, J.M., Pearce, E., Cheever, A., Caulada, Z.A., Caspar, P., Heiny, S., Lewis, F., and Sher, A. (1991). Egg deposition is the major stimulus for the production of Th2 cytokines in murine *Schistosomiasis mansoni*. *J. Immunol.* *146*, 1322–1327.
- Haeberlein, S., Angrisano, A., Quack, T., Lu, Z., Kellershohn, J., Blohm, A., Grevelding, C.G., and Hahnel, S.R. (2019). Identification of a new panel of reference genes to study pairing-dependent gene expression in *Schistosoma mansoni*. *Int. J. Parasitol.* *49*, 615–624.
- Harris, A.R., Russell, R.J., and Charters, A.D. (1984). A review of schistosomiasis in immigrants in Western Australia, demonstrating the unusual longevity of *Schistosoma mansoni*. *Trans. R. Soc. Trop. Med. Hyg.* *78*, 385–388.
- Hartwig, S., Dovengerds, C., Herrmann, C., and Hovemann, B.T. (2014). *Drosophila* Ebony: a novel type of nonribosomal peptide synthetase related enzyme with unusually fast peptide bond formation kinetics. *FEBS J.* *281*, 5147–5158.
- Haseeb, M.A., Eveland, L.K., and Fried, B. (1985). The uptake, localization and transfer of [4–<sup>14</sup>C]cholesterol in *Schistosoma mansoni* males and females maintained *in vitro*. *Comp. Biochem. Physiol. A Comp. Physiol.* *82*, 421–423.
- Hoagland, M.B. (1955). An enzymic mechanism for amino acid activation in animal tissues. *Biochim. Biophys. Acta* *16*, 288–289.
- Hockley, D.J. (1973). Ultrastructure of the tegument of *Schistosoma*. *Adv. Parasitol.* *11*, 233–305.
- Izoré, T., Tailhades, J., Hansen, M.H., Kaczmarek, J.A., Jackson, C.J., and Cryle, M.J. (2019). *Drosophila melanogaster* nonribosomal peptide synthetase Ebony encodes an atypical condensation domain. *Proc. Natl. Acad. Sci. USA* *116*, 2913–2918.
- King, C.H. (2010). Parasites and poverty: the case of schistosomiasis. *Acta Trop.* *113*, 95–104.
- King, C.H., and Dangerfield-Cha, M. (2008). The unacknowledged impact of chronic schistosomiasis. *Chronic Illn.* *4*, 65–79.
- Langenberg, M.C.C., Hoogerwerf, M.A., Koopman, J.P.R., Janse, J.J., Kosvan Oosterhoud, J., Feijt, C., Jochems, S.P., de Dood, C.J., van Schuijlenburg, R., Ozir-Fazalalikhani, A., et al. (2020). A controlled human *Schistosoma mansoni* infection model to advance novel drugs, vaccines and diagnostics. *Nat. Med.* *26*, 326–332.
- Love, M.I., Huber, W., and Anders, S. (2014). Moderated estimation of fold change and dispersion for RNA-seq data with DESeq2. *Genome Biol.* *15*, 550.
- LoVerde, P.T., Andrade, L.F., and Oliveira, G. (2009). Signal transduction regulates schistosome reproductive biology. *Curr. Opin. Microbiol.* *12*, 422–428.
- Lu, Z., Sessler, F., Holroyd, N., Hahnel, S., Quack, T., Berriman, M., and Grevelding, C.G. (2016). Schistosome sex matters: a deep view into gonad-specific and pairing-dependent transcriptomes reveals a complex gender interplay. *Sci. Rep.* *6*, 31150.
- Lu, Z., Spänig, S., Weth, O., and Grevelding, C.G. (2019). Males, the wrongly neglected partners of the biologically unprecedented male-female interaction of schistosomes. *Front. Genet.* *10*, 796.
- Morris, G.P., and Threadgold, L.T. (1967). A presumed sensory structure associated with the tegument of *Schistosoma mansoni*. *J. Parasitol.* *53*, 537–539.
- Pearce, E.J., and MacDonald, A.S. (2002). The immunobiology of schistosomiasis. *Nat. Rev. Immunol.* *2*, 499–511.
- Perrimon, N., Pitsouli, C., and Shilo, B.Z. (2012). Signaling mechanisms controlling cell fate and embryonic patterning. *Cold Spring Harb. Perspect. Biol.* *4*, a005975.
- Pietrobono, S., Gagliardi, S., and Stecca, B. (2019). Non-canonical hedgehog signaling pathway in cancer: activation of GLI transcription factors Beyond smoothed. *Front. Genet.* *10*, 556.
- Popiel, I., and Basch, P.F. (1984). Reproductive development of female *Schistosoma mansoni* (Digenea: Schistosomatidae) following bisexual pairing of worms and worm segments. *J. Exp. Zool.* *232*, 141–150.
- Popiel, I., and Basch, P.F. (1986). *Schistosoma mansoni*: cholesterol uptake by paired and unpaired worms. *Exp. Parasitol.* *61*, 343–347.
- Popiel, I., Cioli, D., and Erasmus, D.A. (1984). The morphology and reproductive status of female *Schistosoma mansoni* following separation from male worms. *Int. J. Parasitol.* *14*, 183–190.
- Richardt, A., Kemme, T., Wagner, S., Schwarzer, D., Marahiel, M.A., and Hovemann, B.T. (2003). Ebony, a novel nonribosomal peptide synthetase for beta-alanine conjugation with biogenic amines in *Drosophila*. *J. Biol. Chem.* *278*, 41160–41166.
- Severinghaus, A.E. (1928). Sex studies on *Schistosoma japonicum*. *Q. J. Microsc. Sci.* *71*, 653–702.
- Shou, Q., Feng, L., Long, Y., Han, J., Nunnery, J.K., Powell, D.H., and Butcher, R.A. (2016). A hybrid polyketide-nonribosomal peptide in nematodes that promotes larval survival. *Nat. Chem. Biol.* *12*, 770–772.
- Singla, V., and Reiter, J.F. (2006). The primary cilium as the cell's antenna: signaling at a sensory organelle. *Science* *313*, 629–633.
- Sotillo, J., Pearson, M., Potriquet, J., Becker, L., Pickering, D., Mulvenna, J., and Loukas, A. (2016). Extracellular vesicles secreted by *Schistosoma mansoni* contain protein vaccine candidates. *Int. J. Parasitol.* *46*, 1–5.
- Stachelhaus, T., Mootz, H.D., and Marahiel, M.A. (1999). The specificity-conferring code of adenylation domains in nonribosomal peptide synthetases. *Chem. Biol.* *6*, 493–505.
- Steinmann, P., Keiser, J., Bos, R., Tanner, M., and Utzinger, J. (2006). Schistosomiasis and water resources development: systematic review, meta-analysis, and estimates of people at risk. *Lancet Infect. Dis.* *6*, 411–425.
- Stenesen, D., Moehlan, A.T., and Krämer, H. (2015). The carcinine transporter CarT is required in *Drosophila* photoreceptor neurons to sustain histamine recycling. *Elife* *4*, e10972.
- Süssmuth, R.D., and Mainz, A. (2017). Nonribosomal peptide synthesis-principles and prospects. *Angew. Chem. Int. Ed. Engl.* *56*, 3770–3821.

- Torres, J.P., and Schmidt, E.W. (2019). The biosynthetic diversity of the animal world. *J. Biol. Chem.* *294*, 17684–17692.
- van der Werf, M.J., de Vlas, S.J., Brooker, S., Looman, C.W., Nagelkerke, N.J., Habbema, J.D., and Engels, D. (2003). Quantification of clinical morbidity associated with schistosome infection in sub-Saharan Africa. *Acta Trop.* *86*, 125–139.
- Wang, H., Fewer, D.P., Holm, L., Rouhiainen, L., and Sivonen, K. (2014a). Atlas of nonribosomal peptide and polyketide biosynthetic pathways reveals common occurrence of nonmodular enzymes. *Proc. Natl. Acad. Sci. USA* *111*, 9259–9264.
- Wang, J., Chen, R., and Collins, J.J. (2019). Systematically improved *in vitro* culture conditions reveal new insights into the reproductive biology of the human parasite *Schistosoma mansoni*. *PLoS Biol.* *17*, e3000254.
- Wang, J., Silva, M., Haas, L.A., Morsci, N.S., Nguyen, K.C., Hall, D.H., and Barr, M.M. (2014b). *C. elegans* ciliated sensory neurons release extracellular vesicles that function in animal communication. *Curr. Biol.* *24*, 519–525.
- Wang, J., Yu, Y., Shen, H., Qing, T., Zheng, Y., Li, Q., Mo, X., Wang, S., Li, N., Chai, R., et al. (2017). Dynamic transcriptomes identify biogenic amines and insect-like hormonal regulation for mediating reproduction in *Schistosoma japonicum*. *Nat. Commun.* *8*, 14693.
- Weinland, D.F., and Wyman, J. (1858). *Human Cestoides : an Essay on the Tapeworms of Man: Giving a Full Account of their Nature, Organization, and Embryonic Development; the Pathological Symptoms they Produce, and the Remedies Which have Proved Successful in Modern Practice* (Metcalf and Company).
- Wendt, G., Zhao, L., Chen, R., Liu, C., O'Donoghue, A.J., Caffrey, C.R., Reese, M.L., and Collins, J.J. (2020). A single-cell RNA-seq atlas of *Schistosoma mansoni* identifies a key regulator of blood feeding. *Science* *369*, 1644–1649.
- WHO (2018). Schistosomiasis and soil-transmitted infections: number of people treated in 2017: Weekly Epidemiological Record (World Health Organization). <https://www.who.int/publications/i/item/who-wer9350>.
- Wright, T.R. (1987). The genetics of biogenic amine metabolism, sclerotization, and melanization in *Drosophila melanogaster*. *Adv. Genet.* *24*, 127–222.
- Ziegler, A.B., Brüsselbach, F., and Hovemann, B.T. (2013). Activity and coexpression of *Drosophila* black with ebony in fly optic lobes reveals putative cooperative tasks in vision that evade electroretinographic detection. *J. Comp. Neurol.* *521*, 1207–1224.

## STAR★METHODS

### KEY RESOURCES TABLE

REAGENT or RESOURCE	SOURCE	IDENTIFIER
<b>Antibodies</b>		
For WISH: Anti-Digoxigenin-AP	Sigma-Aldrich	Cat# 11093274910 RRID:AB_2734716
For FISH: Anti-Digoxigenin-horseradish peroxidase	Roche	Cat# 11207733910 RRID:AB_514500
For FISH: Anti-Fluorescein-horseradish peroxidase	Sigma-Aldrich	Cat# 11426346910
For FISH: Anti-DNP-horseradish peroxidase	Vector Laboratories	Cat# MB-0603-5
<b>Bacterial and virus strains</b>		
MAX Efficiency™ DH10Bac™ Competent Cells for bac-to-bac cloning	Thermo Fisher Scientific	Cat# 10361012
<b>Chemicals, peptides, and recombinant proteins</b>		
ABC169 media supplement: bovine washed red blood cells	Lampire Biological Products	Cat# 7240808
ABC169 media supplement: porcine cholesterol concentrate	Rocky Mountain Biologicals	Cat# PCC-BDG- VCG
ABC169 media supplement: L-ascorbic acid	Sigma-Aldrich	Cat# A5960
Tricaine	Sigma-Aldrich	Cat# A5040
Fast Blue BB	Sigma-Aldrich	Cat# F3378
EdU (5-ethynyl-2'-deoxyuridine)	Invitrogen	Cat# E10187
DAPI	Sigma-Aldrich	Cat# D9542
FAST SYBR Green Master Mix	Bio-rad	Cat# 1725122
cOMplete protease inhibitor	Sigma-Aldrich	Cat# 11873580001
Ni-NTA agarose	Qiagen	Cat# 4561
Strep-Tactin Sepharose resin	Fisher Scientific	Cat# NC9891255
[32P]PP <sub>i</sub>	PerkinElmer	Cat# NEX019001MC
[3H]βAlanine	American Radiolabeled Chemicals	Cat# ART 0205
[13C3]βAlanine	Cambridge Isotope Laboratories	Cat# cIm-8755-PK
βAlanine	Sigma-Aldrich	Cat# 146064
mcBATT	Synthesized by MuseChem, owned by this paper	Batch# M21X01198
swBATT	This paper	Order# MCC-RC-106
<b>Critical commercial assays</b>		
Direct-zol RNA MiniPrep	Genesee Scientific	Cat# 11-330
Illumina TruSeq stranded mRNA library kit	Illumina	Cat# 20020595
iScript cDNA Synthesis Kit	Bio-Rad	Cat# 1708891
<b>Deposited data</b>		
gli1 RNAi RNAseq	GEO	GSE184849
BATT treatment female RNAseq	GEO	GSE191062
Single sex female RNAseq 1	WormBase ParaSite	ERR1328130_1, ERR1328130_2
Single sex female RNAseq 2	WormBase ParaSite	ERR1328191_1, ERR1328191_2
Single sex female RNAseq 3	WormBase ParaSite	ERR1328215_1, ERR1328215_2
Mixed sex female RNAseq 1	WormBase ParaSite	ERR1328194_1, ERR1328194_2
Mixed sex female RNAseq 2	WormBase ParaSite	ERR1328218_1, ERR1328218_2
Mixed sex female RNAseq 3	WormBase ParaSite	ERR1328156_1, ERR1328156_2
<b>Experimental models: Cell lines</b>		
Sf9	ATCC	CRL-1711

(Continued on next page)

**Continued**

REAGENT or RESOURCE	SOURCE	IDENTIFIER
<b>Experimental models: Organisms/strains</b>		
Parasites: <i>Schistosoma mansoni</i>	NIAID Schistosomiasis Resource Center of the Biomedical Research Institute	NMRI
Infected snails: <i>Biomphalaria glabrata</i>	NIAID Schistosomiasis Resource Center of the Biomedical Research Institute	NMRI
Infected female mice	NIAID Schistosomiasis Resource Center of the Biomedical Research Institute	Swiss-Webster
<b>Oligonucleotides</b>		
Forward and reverse primers for riboprobe and dsRNA synthesis	This paper, <a href="#">Table S5</a>	N/A
Forward and reverse primers for qPCR detection	This paper, <a href="#">Table S5</a>	N/A
<b>Recombinant DNA</b>		
pJC53.2- <i>gli1</i> for RNAi and <i>in situ</i> hybridization	This paper	Plasmid# pJW186, Smp_266960
pJC53.2- <i>Sm-nrps</i> for RNAi and <i>in situ</i> hybridization	This paper	Plasmid# pRC90, Smp_158480
pJC53.2- <i>7b2</i> for <i>in situ</i> hybridization	This paper	Plasmid# pLZ180, Smp_073270
pJC53.2- <i>tppp2</i> for <i>in situ</i> hybridization	This paper	Plasmid# pLZ266, Smp_097490
pJC53.2- <i>calp</i> for <i>in situ</i> hybridization	This paper	Plasmid# pGW17, Smp_214190
pJC53.2- <i>tpm2</i> for <i>in situ</i> hybridization	This paper	Plasmid# pLZ93, Smp_031770
pJC53.2- <i>p48</i> for <i>in situ</i> hybridization	This paper	Plasmid# pLZ31, Smp_241610
pJC53.2- <i>bmpg</i> for <i>in situ</i> hybridization	This paper	Plasmid# pLZ262, Smp_078720
Protein expression construct: pFastBac1-His6-StrepII-TEV-SmNRPS, codon optimized to insect cells	This paper	Plasmid# pRC135_OP
Protein expression construct: pFastBac1-His6-StrepII-TEV-SmNRPS_S892A, codon optimized to insect cells	This paper	Plasmid# pRC135.S892A_OP
Protein expression construct: pFastBac1-His6-StrepII-TEV-Ebony	This paper	Plasmid# pRC136, protein NCBI: NM_079707.4
<b>Software and algorithms</b>		
MassHunter Profinder software	Agilent Technologies	Version B.08.00 SP3
T-Coffee sequence alignment	Snappgene 4.3.4	<a href="http://tcoffee.org.cat/">http://tcoffee.org.cat/</a>
MUSCLE sequence alignment	Snappgene 4.3.4	<a href="https://www.ebi.ac.uk/Tools/msa/muscle/">https://www.ebi.ac.uk/Tools/msa/muscle/</a>
STAR	<a href="#">Dobin et al., 2013</a>	N/A
DESeq2	<a href="#">Love et al., 2014</a>	N/A
<b>Other</b>		
40 $\mu$ m cell strainer for female/male worm separation	Thermo Fisher Scientific	Cat# 22-363-547
speed vacuum	Thermo Fisher Scientific	Cat# SPD1010-115
6550 iFunnel Q-TOF mass spectrometer	Agilent Technologies	Cat# G6550BA
Acquity UPLC <sup>®</sup> HSS T3 column	Waters	Cat# 186003539
AB Sciex 6500+ QTRAP <sup>®</sup> mass spectrometer	Framingham	N/A
Nexera X2 UHPLC/HPLC	Shimadzu and Columbia	N/A

**RESOURCE AVAILABILITY**

**Lead contact**

Further information and requests for resources and reagents should be directed to and will be fulfilled by the lead contact, James J. Collins III ([jamesj.collins@utsouthwestern.edu](mailto:jamesj.collins@utsouthwestern.edu)).

**Materials availability**

This study did not generate new or unique reagents. Synthetic BATT can be shared upon request.

### Data and code availability

- Two of the RNA sequencing data sets collected by this study have been deposited at GEO and are publicly available as of the date of publication. Accession numbers are listed in the [key resources table](#). The existing, publicly available data for single sex and mixed sex female RNAseq were obtained from the accession numbers listed in the [key resources table](#). Microscopy data reported in this paper will be shared by the [lead contact](#) upon request.
- This paper does not report original code.
- Any additional information required to reanalyze the data reported in this paper is available from the [lead contact](#) upon request

## EXPERIMENTAL MODEL AND SUBJECT DETAILS

### *S. mansoni* parasites

*S. mansoni* is the Naval Medical Research Institute (NMRI) strain provided by the NIAID Schistosomiasis Resource Center at the Biomedical Research Institute (BRI) (Rockville, MD). Infected *Biomphalaria glabrata* snails (NMRI) and infected mice (Swiss-Webster female mice) were received on a regular basis for parasite recovery and in-house life cycle maintenance. Adult *S. mansoni* were perfused from the hepatic portal vein of mice 6–7 weeks after infection. 37 °C DMEM (Fisher Scientific MT10014CV, NH, USA) with 5% horse serum (Sigma-Aldrich H1138, MO, USA) and heparin was used as perfusion solution. Recovered parasites were washed several times with perfusion solution before culture in BM169 media (Basch, 1981) supplemented with 1 × Antibiotic-Antimycotic (Sigma-Aldrich A5955, MO, USA). Worm pairs were harvested from mice infected with pooled cercaria shed by several *B. glabrata* snails each parasitized with more than 5 miracidia, ensuring a mixed pool of the two sexes. Parasites derived from such infections are referred to as “Mixed Sex”. “Virgin” parasites were harvested from mice infected with cercaria shed by a single snail parasitized by a single miracidium. Adult males which were unpaired for more than 3 days or virgins from single miracidia infections were considered “unpaired”. For regular maintenance, parasites were cultivated in cell culture petri dishes/plates with ~0.5 mL media per worm (pair) at 37°C in 5% CO<sub>2</sub>. Due to the slow metabolism rate of virgin females, ~0.15 mL media/worm was used. Media was changed every other day unless mentioned otherwise. For experiments monitoring reproduction and sexual development, parasites were cultured in ABC169 media (Wang et al., 2019). dsRNA treatment was performed in BM169 unless described otherwise. To separate worm pairs, worms were suspended in BM169 with 0.25% tricaine (Sigma-Aldrich A5040, MO, USA) and agitated for 5 min. Unpaired worms were processed further or washed 2X in BM169 and returned to culture.

### *S. mansoni* infected mice

6–8 week old female Swiss-Webster mice (*Mus musculus*) were infected with cercaria by tail exposure and perfused 6–7 weeks later. Mouse infections were performed either in-house or by BRI. Experiments with and care of mice were performed in accordance with protocols approved by the Institutional Animal Care and Use Committee (IACUC) of UT Southwestern Medical Center (approval APN: 2017-102092).

### *B. glabrata* snails

*B. glabrata* snails of NMRI strain were maintained in artificial pond water (0.125 mg/L FeCl<sub>3</sub>·6H<sub>2</sub>O, 32 mg/L CaCl<sub>2</sub>·2H<sub>2</sub>O, 25 mg/mL MgSO<sub>4</sub>·7H<sub>2</sub>O in pH 7.2 phosphate buffer) and fed with 16% layer chicken feed. For snail infections, livers harvested from “Mixed sex” infected mice were blended and resuspended artificial pond water to liberate miracidia from eggs. Released miracidia were incubated with snails for either “Mixed sex” or “Virgin” infections for 3h and then cultured in artificial pond water until patency.

## METHOD DETAILS

### RNA interference (RNAi)

dsRNA production and RNAi treatment were essentially performed as previously described (Collins et al., 2010, 2013). Oligo sequences used to generate dsRNA templates are listed in [Table S6](#). A dsRNA derived from two bacterial genes was used as a negative control for all RNAi experiments (Collins et al., 2010). D0 represents the first day of the experiment.

For RNAi screening, virgin females were treated with 30 µg/mL dsRNA on D0 in BM169 and then paired with male parasites from D1 onwards in ABC169. Media was supplemented with an additional 30 µg/mL dsRNA on D1/2/6/10 until D14 where phenotypes were monitored. For RNAi treatment of either virgin male or female worms, the unpaired worms were treated with 30 µg/mL dsRNA in BM169 media for one week. After a week, opposite sex worms were added in fresh BM169. The following day, BM169 was replaced by ABC169 for the duration of the experiment. For RNAi experiments in [Figures 1D, 1E, 2A, and 2B](#) (RNAseq), [Figures 3D, 5F, and S4C](#), negative control, *gli1* or *Sm-nrps* dsRNA was added on D0/1/2/3 with fresh media and followed by media change every other day until pairing; for experiments in [Figures 3B and 3C](#), dsRNAs were added every day with media change before pairing. In cases where egg output was quantified, existing eggs were removed from the culture during the last media change (D12 post pairing). Two days later, egg number and the number of female parasites was counted to calculate egg/female/day.

### Parasite/egg staining and imaging

Whole-mount *in situ* hybridization (WISH), fluorescent *in situ* hybridization (FISH) (Collins et al., 2013), Fast Blue BB, DAPI, and EdU labeling (Wang et al., 2019) were performed as previously described. Riboprobes were synthesized from templates generated using primers listed in Table S6. Non-quantitative phenotypes were evaluated by reporting the fraction of worms with a given phenotype/total number of worms examined.

### Gene expression analyses

For RNAseq analysis of *gli1* RNAi-treated worms, dsRNA treatment was performed on male worms for a week at 30  $\mu\text{g/mL}$ , and these male worms were either co-cultured with virgin female parasites separated by 40  $\mu\text{m}$  cell strainers (Fisher Scientific 22-363-547, NH, USA) or allowed to pair for three days in ABC169. Each of the three biological replicates included worms pooled from three technical replicates. Following three days of pairing, worms were separated with 0.25% tricaine in BM169 and collected in Trizol. RNA was extracted using Zymo Direct-zol kit (Genesee Scientific 11-331, CA, USA). The samples were then prepared by Illumina TruSeq stranded mRNA library kit. All 24 samples were sequenced with one flow cell on Illumina NextSeq 550 sequencer with 78bp read lengths. Reads were mapped with STAR (Dobin et al., 2013) and data were analyzed using DESeq2 (Love et al., 2014). Raw and processed data have been deposited in NCBI (GSE184849).

For RNAseq analysis of BATT-treated virgin females, virgin female parasites in six-well plates were separated from equal number of virgin males by 40  $\mu\text{m}$  cell strainer. 5  $\mu\text{M}$  BATT or  $\beta\text{Ala}$  was refreshed every other day with fresh ABC169 media from day0. On day8, females were processed for RNAseq as above. Each of the three biological replicates included worms pooled from two technical replicates. RNA was extracted same as described above. The samples were then prepared using the Illumina TruSeq stranded mRNA library kit. All samples were sequenced on one flow cell on an Illumina NextSeq 550 sequencer with 78bp read lengths. Raw and processed data have been deposited in NCBI (GSE191062). Heatmaps were generated with variance stabilized transformed counts using heatmap in R. The post-pairing transcriptome change analyses were performed from publicly-available paired-end RNAseq data from virgin (single sex) and sexually mature (mixed sex) females (WormBase ParaSite). The accession numbers of the three single sex female biological replicates and the three mixed sex female biological replicates are in the [key resources table](#).

For qPCR analyses, worms were collected in 150  $\mu\text{L}$  Trizol, homogenized, and RNA was extracted using Zymo Direct-zol kit and reverse transcribed with iScript (Bio-rad 1708891, CA, USA). Real time quantitative PCR was performed using FAST SYBR Green Master Mix (Bio-rad 1725122, CA, USA) on a QuantStudio3 real-time PCR system (Fisher Scientific, NH, USA). *cytochrome c* (Smp\_900000) was used as an endogenous control for normalization. The data were analyzed by Applied biosystems on the Thermo Fisher Cloud (Thermo Fisher Scientific, MA, USA).

### Scanning electron microscopy (SEM)

Freshly perfused male worms were rocked gently in BM169 containing 0.25% tricaine for 5 min and beheaded under a light microscope. To relax the male trunks such that the ventral surface was exposed for viewing by SEM, the trunk pieces were then rocked in a gradient of  $\text{MgCl}_2$  diluted in BM169 containing 0.25% tricaine as follows: 0.12 M  $\text{MgCl}_2$  for 30 min, 0.18 M  $\text{MgCl}_2$  for 20 min, 0.3 M  $\text{MgCl}_2$  for 5 min and 0.6 M  $\text{MgCl}_2$  for 1 min). After fixation in 4% formaldehyde in PBS for 30 min, worms were further fixed with 2.5% (v/v) glutaraldehyde in 0.1 M sodium cacodylate buffer overnight at 4  $^\circ\text{C}$ . After three rinses in 0.1 M sodium cacodylate buffer, they were post-fixed with 2% osmium tetroxide in 0.1 M sodium cacodylate buffer for 2 hours. Worms were rinsed with water and dehydrated with increasing concentration of ethanol, followed by increasing concentrations of hexamethyldisilazane in ethanol. Worms were air dried under the hood, mounted on SEM stubs with the ventral surface facing up and sputter coated with gold/palladium in a Cressington 108 auto sputter coater. Images were acquired with a Field-Emission Scanning Electron Microscope (Zeiss Sigma, Jena, Germany) at an accelerating voltage of 10kV.

### Protein expression and purification

SmNRPS or Ebony were expressed in Sf9 cells using the Bac-to-Bac baculovirus expression system (Invitrogen, MA, USA). Codon-optimized DNA of SmNRPS (Genescript, NJ, USA) or original cDNA of Ebony was cloned into pFastBac1 with a His<sub>6</sub> tag, a StrepII tag and a TEV site before the N terminus. Third pass virus (40 mL) was used to infect 1L of Sf9 cells at  $2\text{--}2.5 \times 10^6$  cells/mL. After 72h, cells were centrifuged at 1000 g for 10 min, frozen in liquid N<sub>2</sub> and stored at -80  $^\circ\text{C}$ . Cell pellets were thawed in a 37  $^\circ\text{C}$  water bath and lysed with 60 ml of lysis buffer (20 mM Tris-HCl (pH 8.0), 250 mM NaCl, 5 mM  $\text{MgCl}_2$ , 1% Triton X-100, 0.024 mg/mL DNase, 3 mM 2-mercaptoethanol, 0.2 mM PMSF, Sigma cOmplete protease inhibitor (2 tablet/100 ml) and 10% glycerol for 1 h shaking at 4  $^\circ\text{C}$ . The following steps were performed on ice or at 4  $^\circ\text{C}$ . Lysates were homogenized using a Dounce homogenizer and centrifuged at 45,000 rpm for 50 min. The supernatant was supplemented with 10 mM imidazole (pH 8.0) and incubated with 3 mL equilibrated Qiagen Ni-NTA agarose (50% suspension in lysis buffer) with rotation for at least 1.5 h. The resin was centrifuged at 500 g for 10 min, resuspended with 10 mL supernatant and loaded to a glass chromatography column. The resin was washed with Buffer 1 (20 mM Tris-HCl (pH 8.0), 250 mM NaCl, 5 mM  $\text{MgCl}_2$ , 0.05% Triton X-100, 3 mM 2-mercaptoethanol, 10 mM imidazole (pH 8.0), 1  $\mu\text{g/mL}$  aprotinin, 2  $\mu\text{g/mL}$  leupeptin, 0.2 mM PMSF and 10% glycerol until A<sub>280</sub> in the eluate returned to baseline, followed by Buffer 1 supplemented with 450 mM NaCl and 20mM imidazole. Protein was eluted with Buffer 1 containing 250 mM imidazole. Fractions containing SmNRPS were pooled and applied to a column of 0.9 mL Strep-Tactin Sepharose resin (Fisher Scientific NC9891255, NH, USA) that had been pre-equilibrated with the Ni-NTA elution buffer. The column was washed with 8 mL of 20 mM Tris-HCl

(pH 8.0), 200 mM NaCl, 3 mM MgCl<sub>2</sub>, 0.5 mM DTT and 10% glycerol. SmNRPS was eluted in the same buffer but with only 150 mM NaCl and with 10 mM desthiobiotin. The first 1.8 mL elution was performed immediately. The column was left overnight in 1.8 mL elution buffer followed by elution with 4 more 1.8 mL fractions. Most of the SmNRPS was concentrated in the second fraction. Fractions containing SmNRPS or Ebony according to Coomassie Blue-stained SDS-PAGE were dialyzed against 20 mM Tris-HCl, 150 mM NaCl, 3 mM MgCl<sub>2</sub> and 3 mM DTT, and 10% glycerol) and stored at -80 °C. Protein concentration was estimated by comparison with BSA standards on the same gel.

### Biochemical analysis of SmNRPS

The ATP/PP<sub>i</sub> exchange and βAla unloading assays were adapted from previously reported methods (Hartwig et al., 2014; Richardt et al., 2003). For the exchange assay, each reaction contained 100 μL of 50 mM sodium phosphate buffer (pH 7.0), 25 mM MgCl<sub>2</sub>, 1 mM ATP, 50 μM [<sup>32</sup>P]PP<sub>i</sub> (0.11 cpm/fmol), 0.1 mg/mL BSA, 0.1 mM EDTA, 0.25 μM enzyme and 0.2 mM of the stated amino acid(s). Reactions were incubated at 37 °C for 15 min and quenched with a 1 mL ice cold 1.7% activated charcoal slurry (Millipore Sigma 53663, MA, USA) in 0.1 M Na<sub>4</sub>PP<sub>i</sub> and 0.56 M HClO<sub>4</sub>. Samples were centrifuged at 1000 g for 5 min and the charcoal pellet was washed twice with 1 mL of 5 μM Na<sub>4</sub>PP<sub>i</sub>. Charcoal pellets were resuspended with 0.5 mL deionized water and radioactivity was monitored by scintillation counting.

The unloading assay involves two reaction steps, loading and unloading. In the loading step, 0.25 μM enzyme was first incubated for 30 min at 37 °C in a loading cocktail of 1 mM ATP, 50 mM sodium phosphate (pH 7.0), 25 mM MgCl<sub>2</sub>, 0.1 mg/mL BSA, 0.1 mM EDTA, 5 μM βAla and 10 μCi/mL [<sup>3</sup>H]βAla (American Radiolabeled Chemicals ART 0205, MO, USA). This mixture was chilled on ice. The unloading reaction was initiated by adding 2.22 μL of 100 μM amine to 20 μL of the loading reaction incubation at 37 °C for 10 min. The reaction was then placed on ice, 15 μL of 2.5% (w/v) BSA was added, and protein was precipitated on ice with 10% (w/v) chilled trichloroacetic acid. After 30 min, the solution was transferred to a 1.5 mL conical tube, and centrifuged for 15 min at ~12,000 rpm. The pellet was washed twice with 1 mL of 10% (w/v) chilled trichloroacetic acid, resuspended in 200 μL formic acid, and subjected to scintillation counting. Note that only 2-10% of the enzyme could be loaded with βAla in the initial loading step. This may reflect either inefficient covalent addition of the phosphopantetheinate cofactor in the Sf9 cells (Hartwig et al., 2014), partial denaturation of the enzyme or erroneous estimation of enzyme concentration based on Coomassie Blue staining. Regardless, amounts of loaded enzyme at time zero was normalized to the water unloading control within the same experiment (Figures 4G and 4H).

### Metabolomic analysis

For stable heavy isotope tracing, [<sup>13</sup>C<sub>3</sub>]βAla (Cambridge Isotope Laboratories clm-8755-PK, MA, USA) or normal βAla (Sigma-Aldrich 146064, MO, USA) were added to ABC169 media at 1 mM final concentration and refreshed every other day during media changes for 7 days. Samples of 30 male or female worms were rinsed twice in PBS, flash frozen in liquid N<sub>2</sub>, and homogenized in 1 mL ice-cold 80% methanol in water (vol/vol) using an ultrasonicator (30 s × 3 times at the highest setting). Homogenates were vortexed and 200 μL was diluted in 800 μL ice-cold 80% methanol. This mixture was vortexed again (1 min), centrifuged at maximum speed for 15 min at 4 °C, the supernatant was transferred to new tube, dried overnight using a SpeedVac, and stored at -80 °C. The *in vitro* reaction mix used for the retention time reference of BATT contained 100 μL of 50 mM sodium phosphate buffer pH 7.0, 25 mM MgCl<sub>2</sub>, 0.1 mg/mL BSA, 0.1 mM EDTA, 1 mM βAla, 0.25 mM tryptamine, 5 μM SmNRPS protein and 1 mM ATP. The mixture was incubated at 37 °C for 2.5 h, then added with 1 mL ice-cold 80% methanol, vortexed for 1 min, centrifuged at maximum speed for 15 min at 4 °C. The supernatant was dried to a pellet with a SpeedVac and resuspended in 100 μL deionized H<sub>2</sub>O.

Metabolite analysis data acquisition was performed by reverse-phase chromatography on a 1290 UHPLC liquid chromatography (LC) system interfaced to a high-resolution mass spectrometry (HRMS) 6550 iFunnel Q-TOF mass spectrometer (MS) (Agilent Technologies, CA, USA). The MS was operated in both positive and negative (ESI+ and ESI-) modes. Analytes were separated on an Acquity UPLC® HSS T3 column (1.8 μm, 2.1 × 150 mm, Waters, MA, USA). The column was kept at room temperature. Mobile phase A composition was 0.1% formic acid in water and mobile phase B composition was 0.1% formic acid in 100% ACN. The LC gradient was 0 min: 1% B; 5 min: 5% B; 15 min: 99% B; 23 min: 99% B; 24 min: 1% B; 25 min: 1% B. The flow rate was 250 μL/min. The sample injection volume was 5 μL. ESI source conditions were set as follows: dry gas temperature 225 °C and flow 18 L/min, fragmentor voltage 175 V, sheath gas temperature 350 °C and flow 12 L/min, nozzle voltage 500 V, and capillary voltage +3500 V in positive mode and -3500 V in negative. The instrument was set to acquire over the full *m/z* range of 40-1700 in both modes, with the MS acquisition rate of 1 spectrum s<sup>-1</sup> in profile format. When quantification was required, both samples and BATT concentration standards were spiked with same amount of tryptophan-d<sub>5</sub> as the internal standard.

Raw data files (.d) were processed using Profinder B.08.00 SP3 software (Agilent Technologies, CA, USA) with an in-house database containing retention time and accurate mass information on 600 standards from Mass Spectrometry Metabolite Library (IROA Technologies, MA, USA) which was created under the same analysis conditions. The in-house database matching parameters were: mass tolerance 10 ppm; retention time tolerance 0.5 min; coelution coefficient 0.5. Peak integration result was manually curated in Profinder for improved consistency and exported as a spreadsheet (.csv).

### BATT detection in conditioned media

One worm or worm pair were placed in one well of a 96 well plate with 150 μL ABC169 for two days. Worm pairs were either freshly perfused, freshly separated or separated for 3 days prior to experiment set up. Negative control contained only ABC169 medium.

After 48 hours, 100  $\mu$ L media from each well were sampled and mixed with 100  $\mu$ L methanol containing 0.2% formic acid. The mixtures were vortexed for 15 s, incubated for 10 min at RT and centrifuged at  $\sim$ 18000 g for 5 min. 150  $\mu$ L supernatant was removed to a clean tube and stored at  $-20^{\circ}\text{C}$ . Before analysis, tryptophan-d5 was spiked into the samples as an internal standard. The negative control contained only ABC169 medium. In some experiments, media conditioned by paired worms was collected to evaluate virgin female development. For these experiments,  $\sim$ 10 virgin females were cultured in 1 mL of 48 h pair conditioned media. Every other day, conditioned media was refreshed with media freshly conditioned by worm pairs of the previous 48 hours. Such worms were cultured alongside BATT (5  $\mu$ M) or mock treated virgin females and harvested at day 14.

The BATT concentration was measured in conditioned media by LC-MS/MS using an AB Sciex (Framingham, MA, USA) 6500+ QTRAP<sup>®</sup> mass spectrometer coupled to a Shimadzu (Columbia, MD, USA) Prominence LC. BATT was detected in positive MRM (multiple reaction monitoring) mode by following the precursor to fragment ion transitions of 231.8 to 185.2 (qualifier ion). An Agilent C18 XDB column (5  $\mu$ m, 50 x 4.6 mm) was used for chromatography with the following conditions: Buffer A: H<sub>2</sub>O + 0.1% formic acid; Buffer B: MeOH + 0.1% formic acid; 0–1.5 min 3% B (97% A); 1.5–3.5 min gradient to 100% B (0% A); 3.5–4.5 min 3% B (97% A). Tryptophan-d5 (transition 210.206 to 192.400) was used as internal standard. Concentrations of BATT were determined by comparison to a standard curve prepared by spiking synthetic BATT in DMSO into ABC169 followed by standard sample processing. A limit of detection was defined as a level three times that observed in blank media and the limit of quantitation (LOQ) as the lowest point on the standard curve that gave an analyte signal above the LOD and within 20% of nominal upon back-calculation. The LOQ for BATT was 0.5 ng/mL.

### BATT synthesis and treatment

One batch of  $\beta$ -alanyl-tryptamine (N-(2-(1H-indol-3-yl)ethyl)-3-aminopropanamide) was synthesized by MuseChem (Batch M21X01198, NJ, USA). We refer to this compound as mcBATT. The certificate of analysis showed the purity as 99.88% by HPLC and an ESI-MS confirmed molecular weight of 231.2 g/mol. However, the product was a green, sticky, hygroscopic solid.

We then synthesized a second batch locally (swBATT). The synthesis was a two-step sequence. Boc protected BATT (Boc-BATT, tert-Butyl (3-((2-(1H-indol-3-yl)ethyl)amino)-3-oxopropyl)carbamate) was first synthesized as follows: i-Pr<sub>2</sub>NEt (1.4 mL, 8.0 mmol) was added to a solution of Boc- $\beta$ -Ala-OH (1.0 g, 5.29 mmol), tryptamine (851.9 mg, 5.32 mmol) and HATU (2.42 g, 6.4 mmol) in DMF (24 mL) in a 50 mL round bottom flask. The reaction was stirred overnight and the reaction went to completion as judged by HPLC/MS analysis. Water was added to the reaction mixture, which was then extracted with EtOAc. The organic layer was washed several times with water and then with brine, dried over Na<sub>2</sub>SO<sub>4</sub>, filtered and condensed. The crude mixture was purified via ISCO flash chromatography in 1-10% MeOH/DCM to give 1.55 g of the Boc-BATT in 88% yield. For the second step, TFA (1.0 mL) was added dropwise to a solution of Boc-BATT (497.5 mg, 1.5 mmol) in 10 mL DCM in a scintillation vial. The reaction went to completion within 2 hours and was thereafter condensed under reduced pressure. The crude mixture was purified by reverse phase ISCO flash chromatography in 0-40% H<sub>2</sub>O/CH<sub>3</sub>CN. Fractions containing the desired product were combined and condensed on a speed vacuum (Thermo Fisher Scientific SPD1010-115, MA, USA) to give 505.4 mg of the TFA salt (98% yield). Proton NMR was performed on both Boc-BATT and the final product, swBATT, for confirmation. This product was a brown, extremely hygroscopic, oil-like compound.

Concentrated stock solutions of mcBATT or swBATT were prepared in sterile filtered deionized water and stored at  $< -20^{\circ}\text{C}$ . Because of the hygroscopic nature of both preparations and the unexpected colors, we estimated the concentration of stock solutions by UV absorbance in comparison to solutions of tryptamine after extensive dilution. Concentrated aqueous solutions of BATT displayed broad absorbance maxima above 300 nm, consistent with their appearance. Upon further dilution, the absorbance maxima sharpened and shifted to the UV such that  $< 1$  mM BATT from either batch displayed an absorbance spectrum with a 240-300 nm spectrum essentially identical to that of tryptamine. The colors of the semi-solid and concentrated solutions thus appear to result from stacking of the indole rings. For treatment of worms, the compound was directly added into ABC169 media to achieve desired concentration. Compound was refreshed every other day with fresh media.

### QUANTIFICATION AND STATISTICAL ANALYSIS

For RNAseq experiments, base calling was performed by Illumina cassava 1.9 software. Sequenced reads were trimmed for adaptor sequence, and masked for low-complexity or low-quality sequence, then mapped to the *S. mansoni* genome (v7) using STAR (Dobin et al., 2013). Pairwise comparisons of differential gene expression were performed with DESseq2 (Love et al., 2014). For statistical analysis of non-sequencing data, GraphPad Prism software processed and presented the data as the mean with SD. Statistical significance was calculated by unpaired two-tailed parametric *t* test. Unpaired ordinary one-way ANOVA was also performed in Figure 4G. P values  $< 0.05$  are considered significant (NS, not significant; \*,  $p < 0.05$ ; \*\*,  $p < 0.01$ ; \*\*\*,  $p < 0.001$ ; \*\*\*\*,  $p < 0.0001$ ).

# Supplemental figures

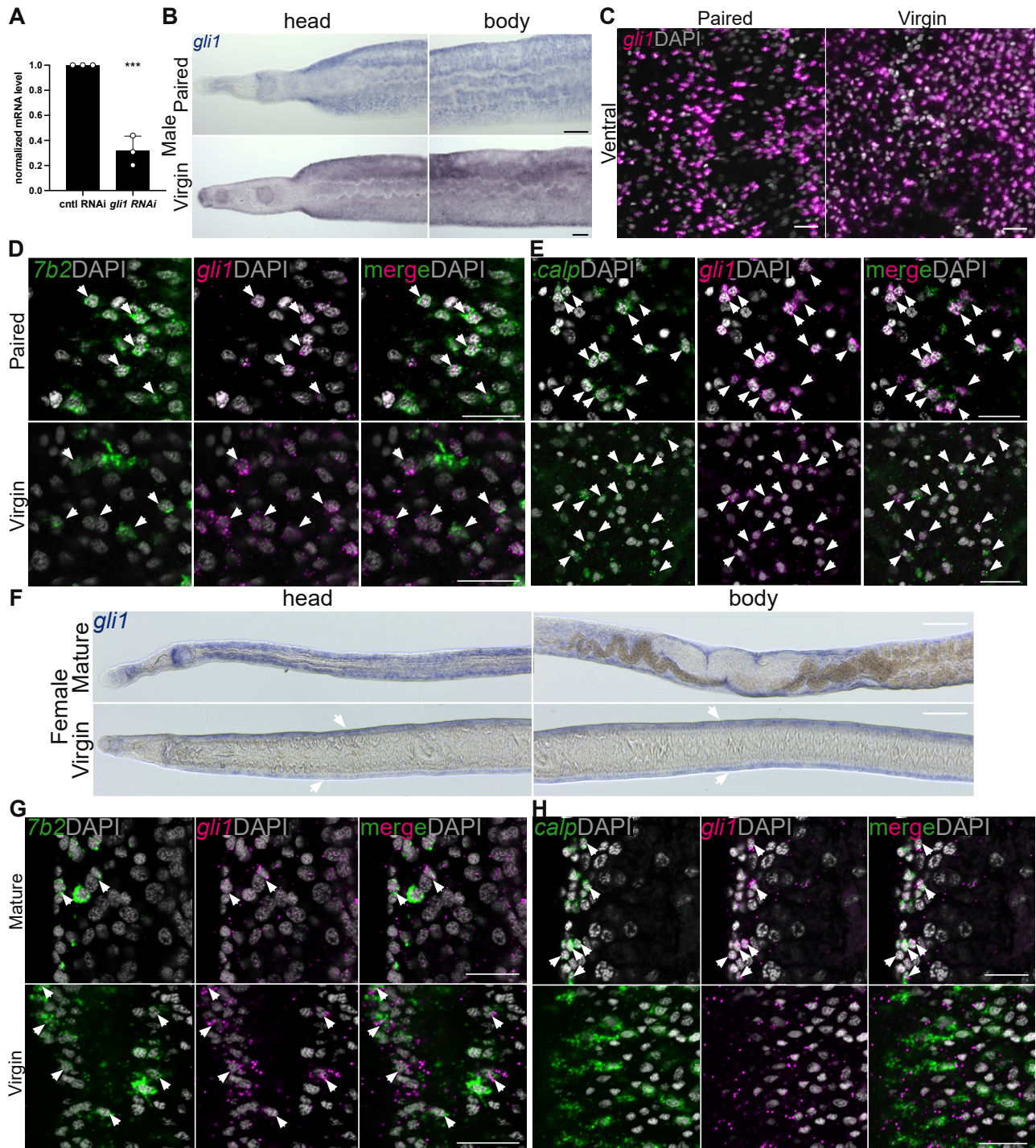


**Figure S1. *gli1* mRNA is expressed in male and female tegumental and neuronal cells, related to Figure 1**

(A) qPCR showing the relative mRNA level of *gli1* in cntl RNAi or *gli1* RNAi males at the end of 2 weeks of pairing. \*\*\*  $p < 0.001$ . Parametric t test. Data from three biological replicates.

(B) Whole-mount colorimetric *in situ* hybridization showing expression of the *gli1* gene in a paired male worm (top) and a virgin male worm (bottom).

(legend continued on next page)

---

(C) FISH showing the expression of *gli1* (magenta) mRNA in the ventral region of paired and virgin males.

(D) Two-color FISH for *7b2* (green) and *gli1* (magenta) mRNAs in paired (top) or virgin (bottom) male worms.

(E) Two-color FISH for *calp* (green) and *gli1* (magenta) mRNAs in paired (top) or virgin (bottom) male worms.

(F) Whole-mount colorimetric *in situ* hybridization showing expression of the *gli1* gene in a sexually mature female worm (top) and a virgin female worm (bottom). Arrows indicate *gli1* mRNA expression in virgin female.

(G) Two-color FISH for *7b2* (green) and *gli1* (magenta) mRNAs in sexually mature (top) or virgin (bottom) female worms.

(H) Two-color FISH for *calp* (green) and *gli1* (magenta) mRNAs in sexually mature (top) or virgin (bottom) female worms. For (E, G, and H), arrows indicate co-expression. All images are representative of 3 experiments with  $n > 10$ . DAPI, gray. Scale bars, 100  $\mu\text{m}$  in (B and F) and 20  $\mu\text{m}$  in (C–E, G, and H).

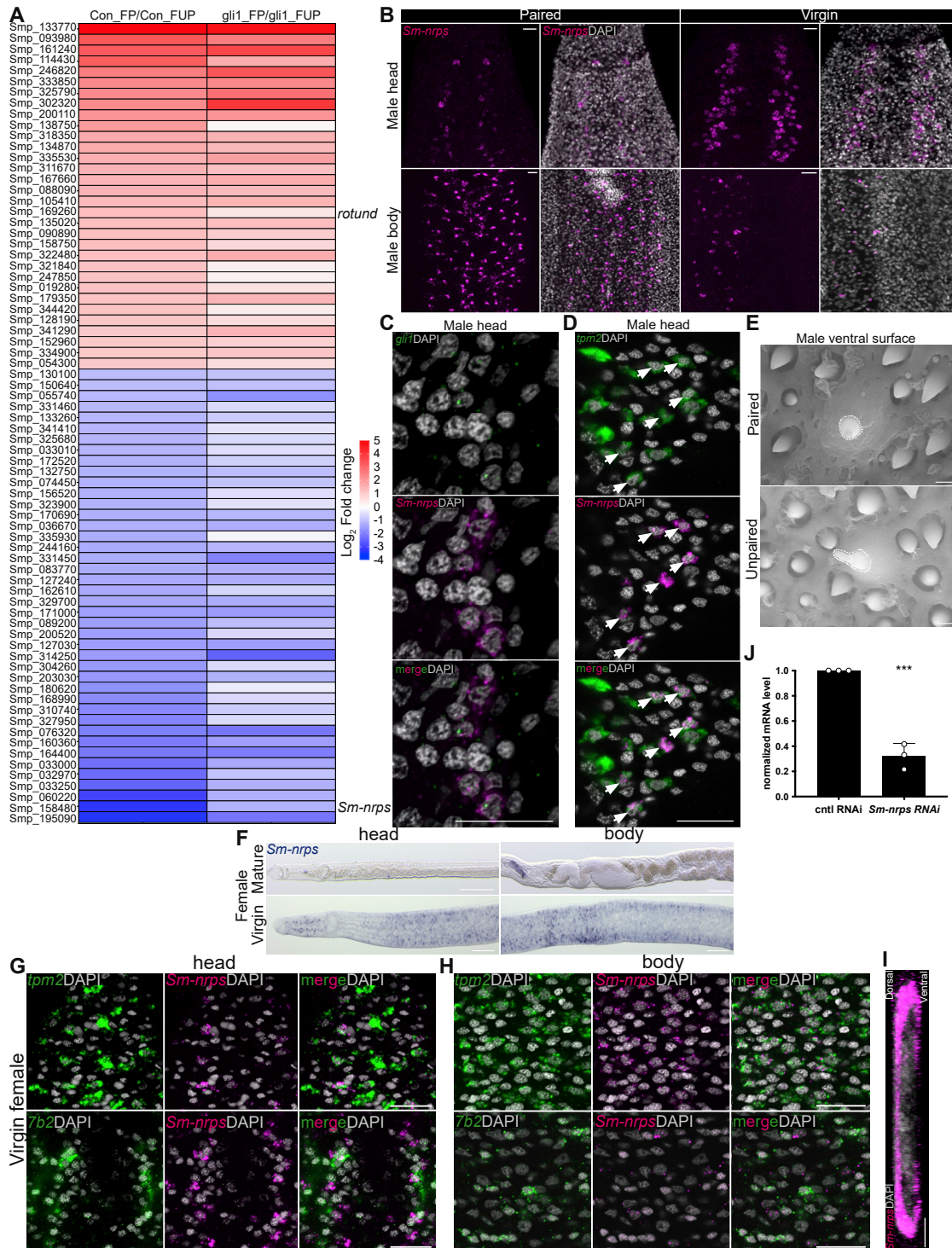


**Figure S2. *Sm-nrps* gene expression in male and female worms, related to Figures 2 and 3**

(A) Heatmap of upregulated and downregulated genes in females after pairing with cntl RNAi males or *gli1* RNAi males. Con\_FP, virgin females paired with cntl RNAi males; Con\_FUP, virgin females left unpaired and cocultured cntl RNAi males; gli1\_FP, virgin females paired with *gli1* RNAi males; gli1\_FUP, virgin females left unpaired and cocultured with *gli1* RNAi males. Genes limited to those with 2-fold change and adjusted p value < 0.0001 of Con\_FP/Con\_FUP.

(B) FISH showing head and body expression of *Sm-nrps* mRNA (magenta) in the male parasites in paired and virgin worms.

(C and D) Two-color FISH for (C) *gli1* or (D) the muscle marker *tpm2* with *Sm-nrps* in the head of virgin male parasites. Arrows indicate cells coexpression.

(legend continued on next page)

---

(E) Scanning electron microscopy showing the ventral surface of a paired male parasite and an unpaired male parasite. White-dotted lines enclose a sensory cilium-like structure. Representative images from 3 parasites.

(F) Whole-mount colorimetric *in situ* hybridization showing expression of the *gli1* gene in a sexually mature female worm (top) and a virgin female worm (bottom).

(G and H) Two-color FISH for *tpm2* or *7b2* with *Sm-nrps* mRNAs in the (G) head or (H) body of a virgin female parasite.

(I) Confocal sagittal section of *Sm-nrps* FISH (magenta) showing mRNA enriched in the dorsal surface and the body edges of a virgin female worm.

(J) qPCR showing relative *Sm-nrps* levels following RNAi treatment in male worms 2 weeks postpairing. \*\*\* $p < 0.001$ . Parametric t test. Data from three biological replicates. All FISH and WISH images are representatives of data from 3 experiments with  $n > 10$  parasites. DAPI, gray. Scale bars: 20  $\mu\text{m}$  in (B–D and G–I), 0.5  $\mu\text{m}$  in (E), and 100  $\mu\text{m}$  in (F).

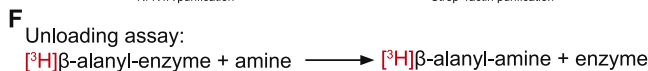
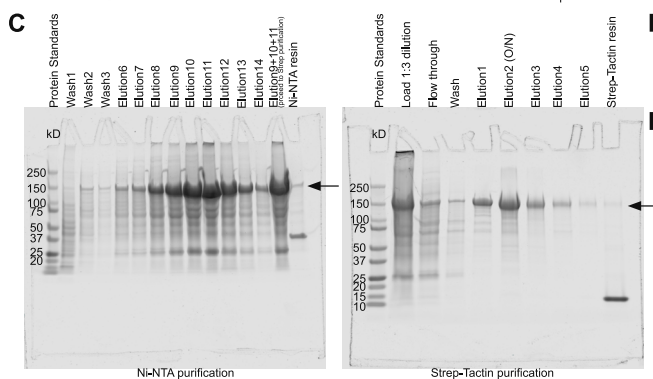
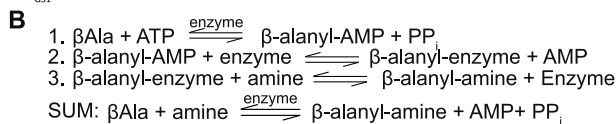
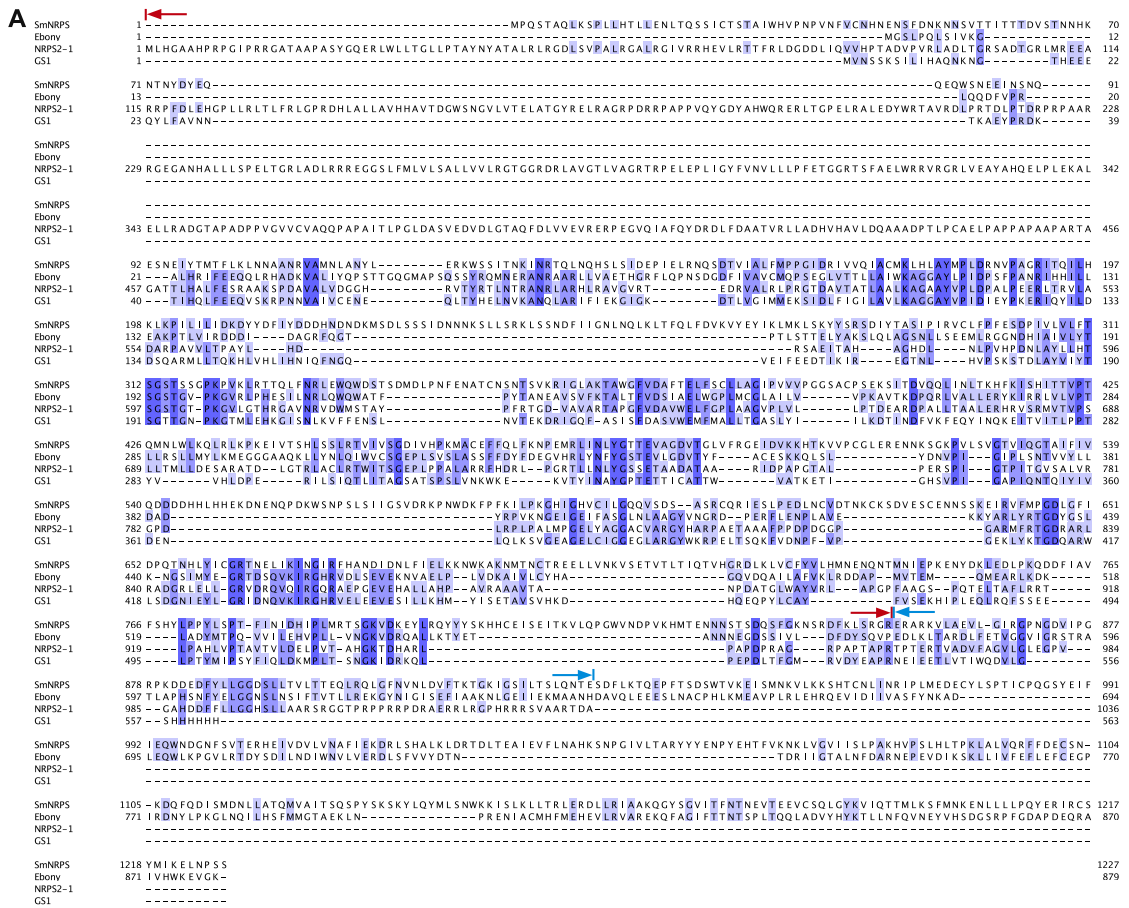


**Figure S3. SmNRPS-catalyzed production of β-alanyl-bioamines, related to Figure 4**

(A) MUSCLE alignment of NRPS enzymes. SmNRPS and Ebony represent full-length protein sequences. NRPS2-1 includes the first A and the following T domain encoded from the *blmIV* gene. GS1 is the A domain from *gramicidin synthetase 1*. The region within the red arrows represents the A domain whereas the region in the blue arrows is the T domain.

(B) Enzymatic reactions performed by Ebony and SmNRPS.

(legend continued on next page)

---

(C) SDS-PAGE gel images of fractions from SmNRPS protein purification. The Elution2 fraction from Strep-Tactin purification was dialyzed against the storage buffer and used for assays. Arrows point to where SmNRPS bands migrate (~150 kDa).

(D) Reaction for ATP-PP<sub>i</sub> exchange assay. The assay measures the reverse reaction by the production of [<sup>32</sup>P] ATP from [<sup>32</sup>P]PP<sub>i</sub>.

(E) ATP-PP<sub>i</sub> exchange assay with *Drosophila* Ebony and SmNRPS. \*\*\*\*p < 0.0001. Parametric t test. Error bars are SD.

(F) Reaction for unloading assay. Bioamine reacts with the covalently [<sup>3</sup>H]βAla-labeled enzyme to release free enzyme.

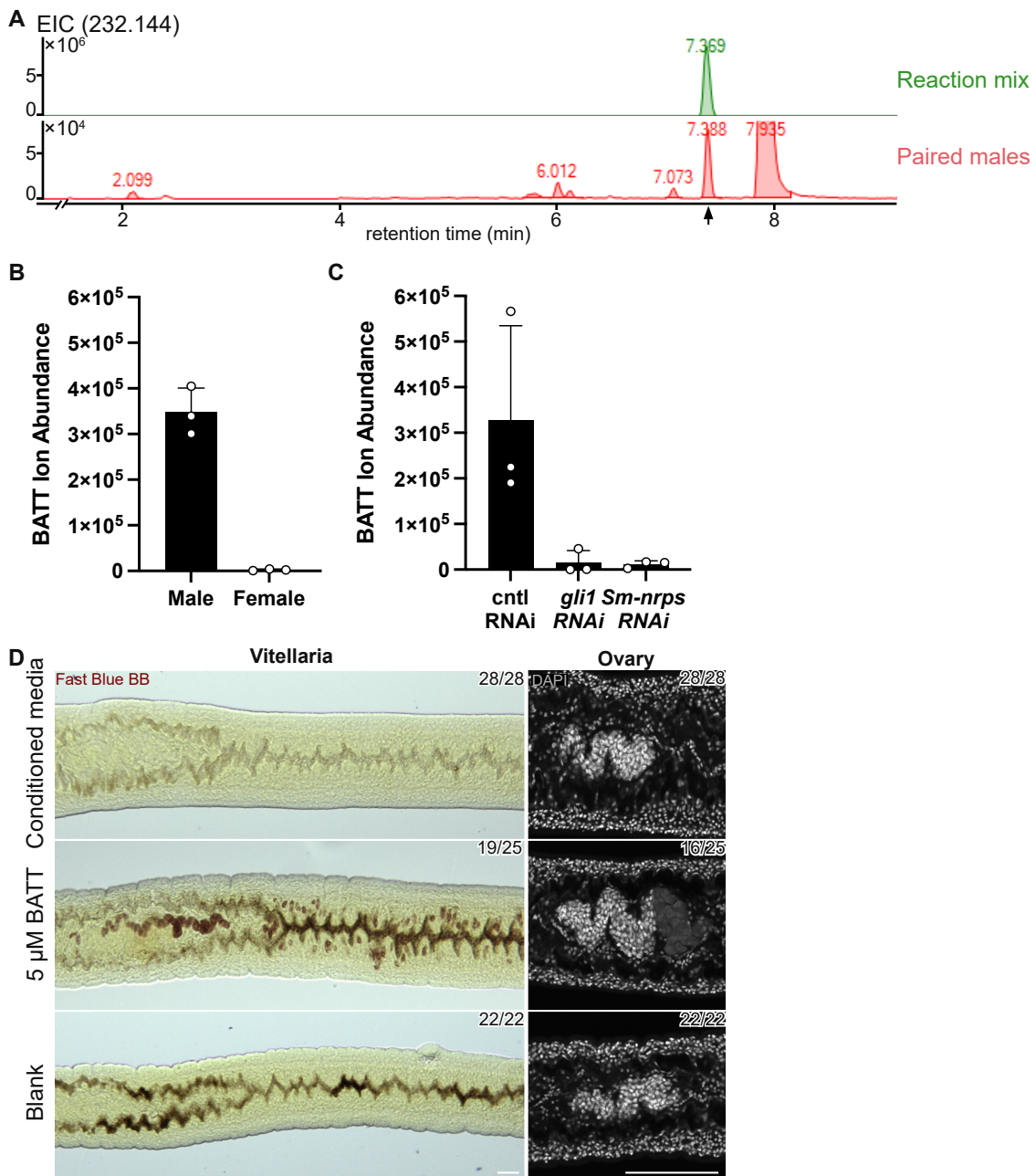


**Figure S4. Unlabeled BATT abundance in the  $[^{13}\text{C}_3]\beta\text{Ala}$  tracing experiments, related to Figure 5**

(A) LC/MS extracted-ion chromatogram (EIC) of  $m/z$  at 232.144 showing retention time of BATT from paired male extracts (bottom) and an *in vitro* reaction mixture (top) containing SmNRPS,  $\beta\text{Ala}$ , tryptamine, ATP, and magnesium. Paired male data show a sample extracted from paired worms exposed to control RNAi. y axis is ion abundance, and x axis is retention time from 1.5 to 8.5 min. Time is shown for all peaks.

(B) LC-MS showing abundance of BATT in paired male and female parasites.

(C) LC-MS showing BATT abundance following RNAi treatment in paired male worms.

(D) Images of Fast Blue BB (left) and DAPI (right) staining 14 days after exposure of virgin females to male:female conditioned media (same in Figure 5H), 5  $\mu\text{M}$  BATT and no treatment. Representative images from 3 experiments with  $n > 22$  worms. Numbers in corner indicate fraction of worms similar to those presented/total number of worms examined. Scale bars, 100  $\mu\text{m}$ .

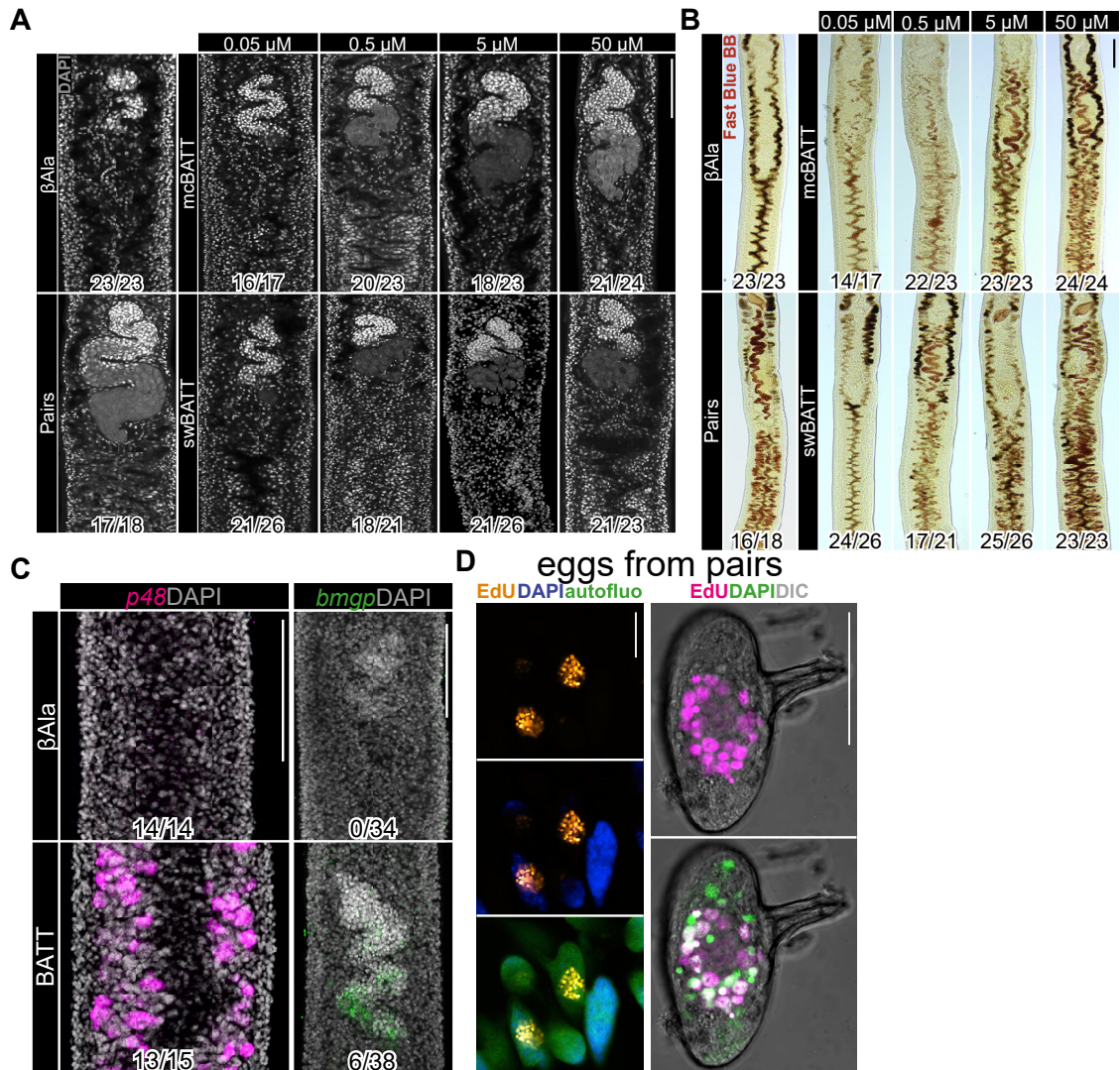


**Figure S5. Two independent sources of BATT stimulate virgin female parasites to sexually mature, related to Figure 6**

(A) DAPI staining of virgin females after 14 days of 0.05–50  $\mu$ M mcBATT or swBATT treatment; 100  $\mu$ M  $\beta$ Ala treatment was used a control.

(B) Fast Blue BB (red) staining of virgin females after 14 days of 0.05–50  $\mu$ M mcBATT or swBATT treatment, 100  $\mu$ M  $\beta$ Ala treatment was used a control. In (A and B) are from the same experiments as data shown in Figure 6E.

(C) FISH for *p48* (magenta) in the vitellaria and *bmgp* (green) of in the ovary of virgin females after 14 days of 50  $\mu$ M mcBATT or  $\beta$ Ala treatment.

(D) (Left) EdU staining (gold) of eggs laid by virgin female worms 14 days after pairing with a male. Autofluorescence (autofluo, green) shows egg shape. (right) Confocal micrograph of EdU labeling and differential interference contrast (DIC) of an egg with laid by a virgin female worm 14 days after pairing.

(A and B) Representative images from 3 experiments with  $n > 18$ .

(C) Representative images from 3 experiments with  $n > 14$  worms. Numbers in corner indicate fraction of worms similar to those presented/total number of worms examined. Scale bars, 100  $\mu$ m.

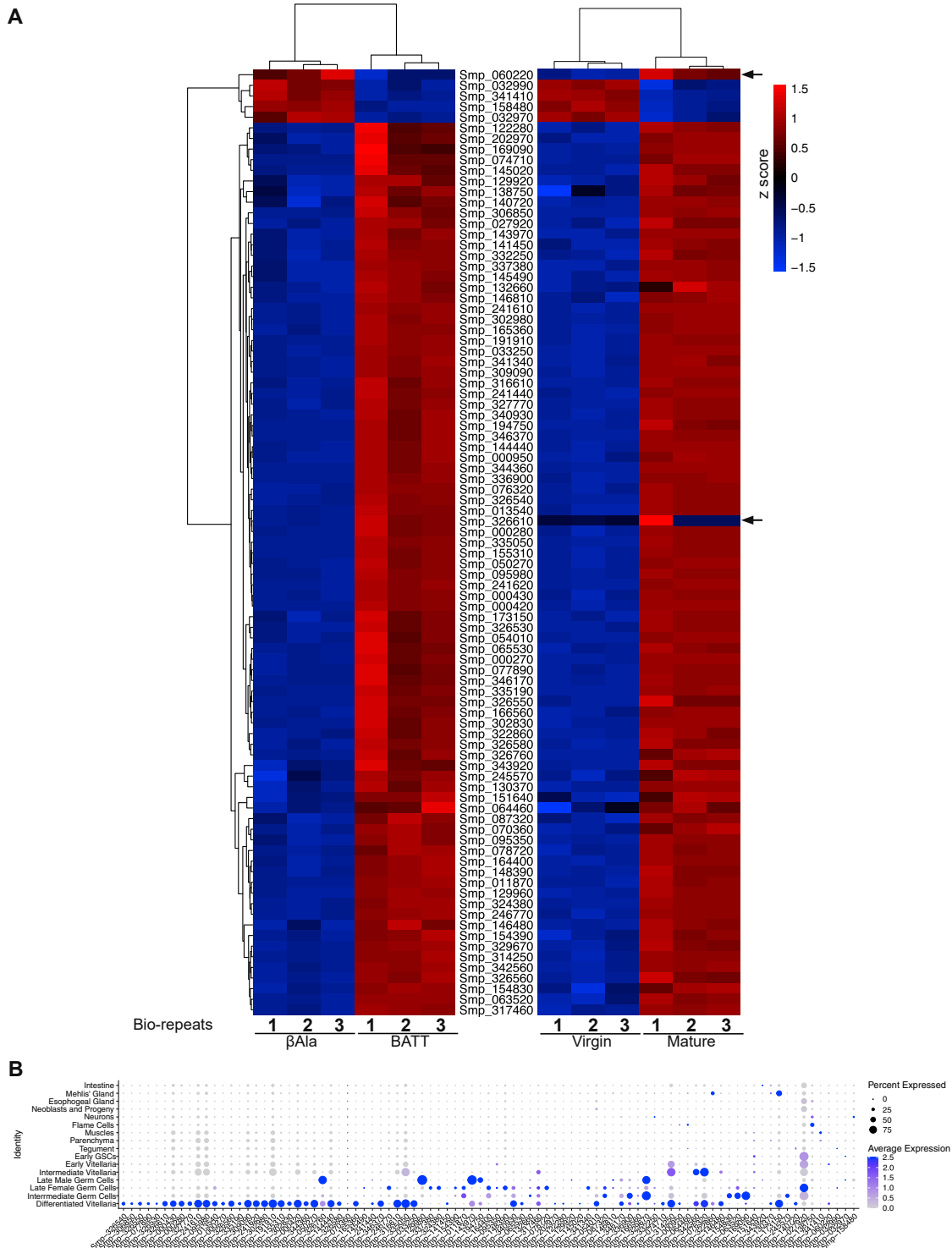


**Figure S6. Gene expression changes in virgin females after 8-day treatment with 5  $\mu$ M BATT, related to Figure 6**

(A) Left, hierarchal clustered heatmap of 89 genes differentially regulated following BATT treatment ( $\log_2$  fold change  $> \pm 2$ , adjusted  $p < 0.05$ , base mean  $> 50$ ). The expression of these same 89 genes were evaluated in publicly available RNA-seq data from virgin and sexually mature female parasites (right). Arrows indicate two instances where gene expression trend was different between two datasets. Accession numbers of virgin and sexually mature female data can be found in [key resources table](#).

(legend continued on next page)

---

(B) Dot plot showing expression of the 89 BATT-regulated genes across scRNA-seq clusters from adult parasites (Wendt et al., 2020). Each row represents a cluster type and each row a gene. Size of circles and color reflect percentage of cells expressing marker and the level of expression, respectively. For ease of visualization, in some cases clusters, related cell types were collapsed into a single cluster. (e.g., 31 clusters of neurons and 8 clusters of muscles were reduced to single cluster.)

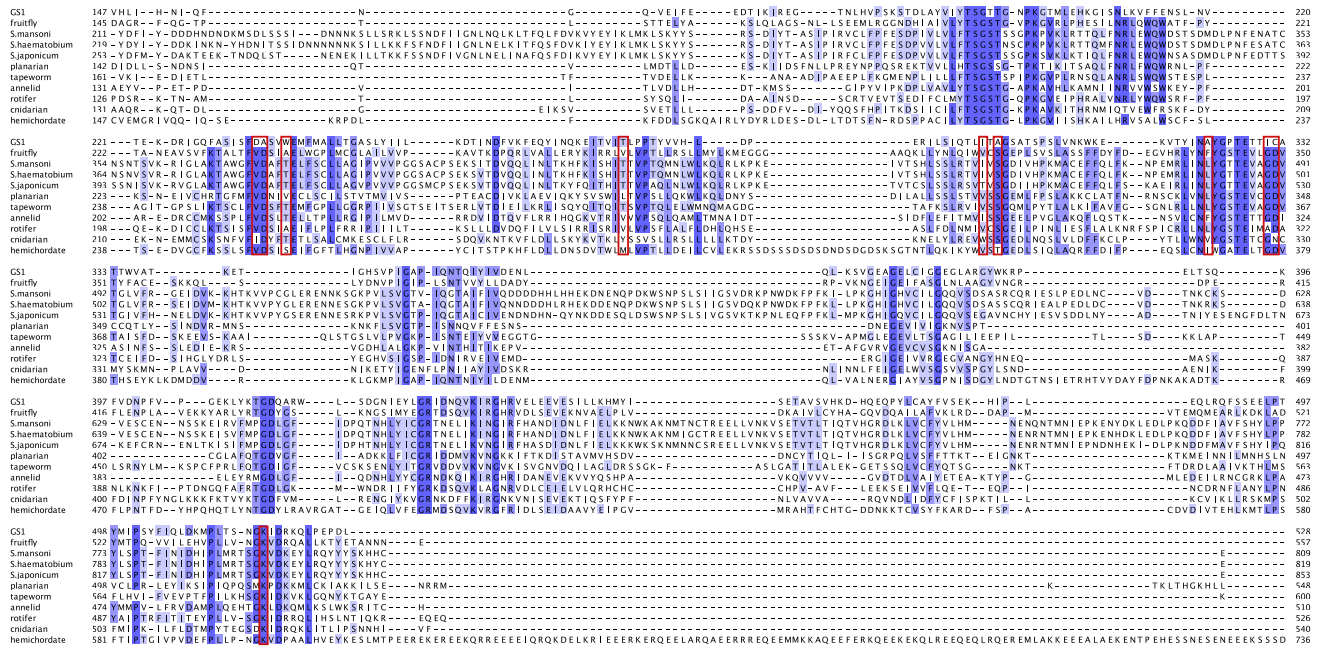


**Figure S7. Alignment of SmNRPS with A domains of related enzymes from different metazoan organisms, related to Figure 7**

Multiple sequence alignment of A domains from NRPS enzymes. Residues aligned to those involved in amino acid specificity in the reference Phe-specific A domain of GS1 are marked in red rectangles. Fruit fly, *Drosophila melanogaster*; *S. mansoni*, *Schistosoma mansoni*; *S. haematobium*, *Schistosoma haematobium*; *S. japonicum*, *Schistosoma japonicum*; planarian, *Schmidtea mediterranea*; tapeworm, *Hymenolepis diminuta*; annelid, *Capitella teleta*; rotifer, *Rotaria magnacalcarata*; cnidarian, *Hydra vulgaris*; and hemichordate, *Saccoglossus kowalevskii*. Alignment was analyzed using T-Coffee. Aligned amino acids were colored by percentage identity (dark blue, 100%; white 0%).